``

Aircraft and Rotorcraft Conceptual Design: Design Trends for the Preliminary Sizing and Surrogate Models for Performance Estimation.

Author

Shoaib Sultan

Regn Number

00000275486

Supervisor

Dr. Shahid Ikram ullah Butt

DEPARTMENT

SCHOOL OF MECHANICAL & MANUFACTURING ENGINEERING

NATIONAL UNIVERSITY OF SCIENCES AND TECHNOLOGY

ISLAMABAD

AUGUST 2022

``

Aircraft and Rotorcraft Conceptual Design: Design Trends for the Preliminary Sizing and Surrogate models for Performance Estimation.

Author

Shoaib Sultan

Regn Number

00000275486

A thesis submitted in partial fulfillment of the requirements for the degree of

MS Mechanical Engineering

Thesis Supervisor:

Dr. Shahid Ikram ullah Butt

Thesis Supervisor's Signature: _____

DEPARTMENT

SCHOOL OF MECHANICAL & MANUFACTURING ENGINEERING

NATIONAL UNIVERSITY OF SCIENCES AND TECHNOLOGY,

ISLAMABAD

AUGUST 2022

``

Declaration

I certify that this research work titled "*Aircraft and Rotorcraft Conceptual Design: Design Trends for the Preliminary Sizing and Surrogate models for Performance Estimation."* is my work. The work has not been presented elsewhere for assessment. The material that has been used from other sources it has been properly acknowledged / referred.

Signature of Student

Shoaib Sultan

``

Plagiarism Certificate (Turnitin Report)

This thesis has been checked for Plagiarism. Turnitin report endorsed by Supervisor is attached.

Signature of Student

SHOAIB SULTAN

Registration Number

00000275486

``

Copyright Statement

``

Acknowledgments

I would like to show my gratitude to many people for helping me complete this challenging thesis, that I am truly proudly of.

First and foremost, thanks to Allah Almighty for bestowing me with this opportunity to study in this premier institute with perseverance and diligence.

Secondly, I would like to show gratitude to Dr. Adnan Maqsood, who has been a beacon of guidance throughout my struggle. Without his constant motivation and support, this incredible feat would not have been possible. His knowledge of the field has benefitted me in ways beyond words.

I am indeed forever indebted to my parents for their constant struggle, unwavering faith and limitless prayers, who left no stone unturn to help me reach to this level.

I also would like to thank my siblings for their love and support no matter what. Lastly, my friends who have been motivating and uplifting me throughout this journey.

``

Dedicated to my exceptional parents and adored siblings whose tremendous support and cooperation led me to this wonderful accomplishment.

``

Abstract

This research discusses the development of surrogate models for aircraft and rotorcraft design during the conceptual phase. The approach proposed in this study, on a crude scale, holds a strong utilization potential among the design community and aero modelers during the preliminary sizing. The fixed-wing aircraft database includes fighters, trainers, transport aircraft, agricultural planes, amphibious aircraft, light utility planes, motor-gliders, sport planes, and freighters. Similarly, the rotorcraft database comprises conventional, fenestron, counter-rotating, and no tail rotor configurations was developed from commercially available data. Linear/Non-Linear regression modeling using power laws is carried out to explore highly correlated design trends among aircraft and rotorcraft weight, geometric, propulsion, and performance parameters. These design trends identify interdependencies among design parameters and provide initial design bounds for preliminary sizing. Aircraft and rotorcraft design is complex process, and a single variable can never predict the response with adequate confidence. Surrogate models using multiple linear regression techniques were developed to estimate aircraft and rotorcraft performance parameters: range, rate of climb, service ceiling, and maximum velocity. Moreover, these models are validated using a two-step process that includes verifying each model using quantitative criteria and checking the prediction accuracy of each model.

Key Words: *Surrogate Models, Design Trends, Aircraft design, Rotorcraft Design, Single Variable Models, Multivariable Models.*

``

Table of Contents

``

``

List of Figures

``

List of Tables

``

CHAPTER 1: **INTRODUCTION**

The research work in this dissertation is divided into three main parts. In the first part, a single variable modeling technique is used to explore highly correlated, significant design trends for both the rotorcraft and the fixed-wing aircraft. The second part focuses on surrogate modeling of aircraft/rotorcraft performance parameters using a multivariable modeling approach. Finally, the third part of the thesis is dedicated to Biomimicry, which includes a detailed discussion of nature-inspired solutions in the aerospace and non-aerospace domain and the comparative study of the scaling properties of natural and man-made flyers.

1.1 Background, Scope, and Motivation

The elegance of the power-law stems from the fact that it appears widely in physics, biology, planetary and earth science, computer science, demography, social science, economics, finance, etc. It is both alluring and intriguing that from the distribution of sizes of cities, earthquakes, moon crates, publications, citations, hits on a webpage, species in biological taxonomy, people annual income to people personal fortunes all follow power-law distribution [1]. The most recent and comprehensive scalability studies conducted by Geoffrey West [2, 3] contain relationships in almost every field of life, ranging from animal metabolic rates to life in big cities. These studies capture the complex scaling trends through simple power-law "$Y = \alpha * X^{\beta}$ " with the exponents that are simple multiples of ¼ (for example, ¼, ¾, etc.). Similarly, several scalability studies have been conducted to find the relationships among different parameters in technology. Moore's Law [4], proposed in 1965, was one of the most prominent among them. It established a relationship that the number of transistors in a dense electronic circuit will double approximately every two years. The prediction remained accurate for several decades. The transistor industry followed the law by bringing improvements in central processing units (CPUs). Although the performance improvement through CPUs has ceased to follow Moore's law, the industry is still chasing the law through graphical processing units (GPUs).

Scaling laws, developed through simple statistical techniques, have produced astounding results. The results deduced from the statistical approach are pretty much comparable with analytical

``

solutions and can be instrumental in building surrogate models. These statistical techniques are used in various contexts, from predicting human behavior to estimating machine performances.

Tennekes [5] explained the elegance of scaling law in the realm of aeronautics through "The Great flying diagram." The diagram is constructed using the weight, cruise velocity, and wing loading. The scope of the graph extends from the smallest bird that is the "common fruit fly," weighing about 7.6×10^{-6} N at one end, to the one of largest aircraft, Boeing 747, weighing about 3.5×10^{6} N at the other end. The size comparison between the two is immense, where Boeing 747 is 460 billion times heavier and about 250 million times larger in terms of wing area. Despite these enormous size differences, the cruise velocity of the Boeing 747 is only 200 times greater. The deductions of "The Great Flying Diagram" are unique and an eye-opener as it put bounds on the aviation designs which are yet to be explored by humans.

``

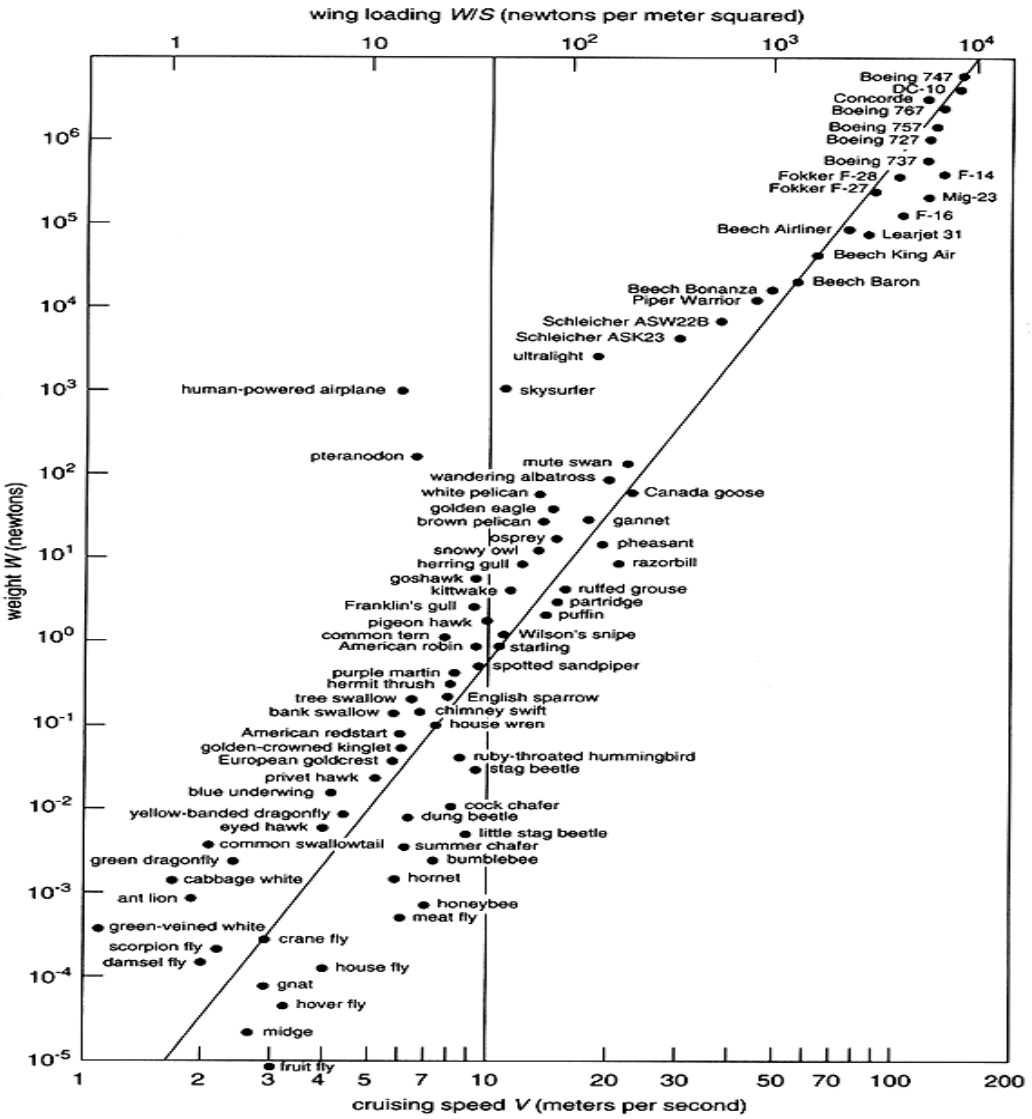

Figure 1-1: The Great Flying Diagram

The diversity in natural and man-made flyers can be captured through scaling laws. The minor deviations are typically attributed to the design versatilities that show restricted freedom available to the designers. The designs that are away from the underlying scaling trends need either more muscle strength or power to remain in the air, resulting in either low endurance or muscle exhaustion.

Aircraft/rotorcraft design is a complex and iterative process; it mainly consists of three phases: conceptual design, preliminary design, and detailed design. Conceptual design starts with customer requirements, which are then translated into concept sketch based on new concept ideas and the availability of technology. Concept sketches are then forwarded for initial sizing,

``

including geometric sizing, engine matching, preliminary weight estimation, etc. The primary goal of the conceptual design phase is to determine the overall shape, size, weight, and performance of the design to a somewhat fuzzy latitude [6]. In the preliminary design phase, minor changes in design layout (if any) are carried out, followed by detailed performance, structural, and control system analysis. The final stage is the detailed design in which every single component of the design, from the nuts and bolts to the tools and jigs, is precisely designed.

In conclusion, the conventional fixed-wing aircraft design process includes defining detailed geometric descriptions, and estimating aerodynamic data from rigorous computational, analytical, or experimental techniques, followed by aircraft performance modeling using point-mass models. The whole process sometimes gets tedious, especially when the design activity is undergoing several iterations. It gets cumbersome most of the time, and the results achieved in the end are still approximates. The designers, over decades, have come up with different designs following the same fundamental abstract principles. We now have enough data on different aircraft to generate approximate/surrogate models from past designs. The initial design process is iterative and requires validation from analytical/computational methods before the design goes into the experimental phase. The solution needs to be well optimized before the sketch goes into prototyping, as the financial blows from a failed prototype are enough to shelf the whole project. Aviation history is witness to the fact that flaws were overlooked in the design phase and resulted in prototyping failing, thus jeopardizing the entire project. The solution to this problem lies in efficiently optimizing the initial design so that later details can be studied thoroughly. In this regard, the proposed research contributes to the overall design process in the following manner:

Firstly, aircraft/rotorcraft design is more evolutionary than a revolutionary process. Most of the future designs are built on past designs; it is thus vital that pre-existing trends are analyzed closely and all influencing parameters for the new aircraft are examined appropriately. In this regard, design trends would allow design engineers to better understand design restrictions and potential design perspectives. In addition to that, design trends, in conjunction with pre-existing semi-empirical relations, can be used as prediction and estimation tools for the initial sizing of aircraft/rotorcraft weight, thrust/power, and geometric parameters. Secondly, surrogate models are quick, easy, and efficient tools to estimate aircraft/rotorcraft performance parameters during

``

the initial design phase. However, it is to be noted that surrogate models are low-fidelity in nature and are designed to complement pre-existing techniques by providing zeroth- or first-order performance estimations upon which later design phases may improve. Therefore, high-fidelity tools must be used to calculate aircraft performance parameters more precisely in the latter stages of the design process.

The research contribution in conceptual aircraft/rotorcraft design is further summarized in figure 1.2.

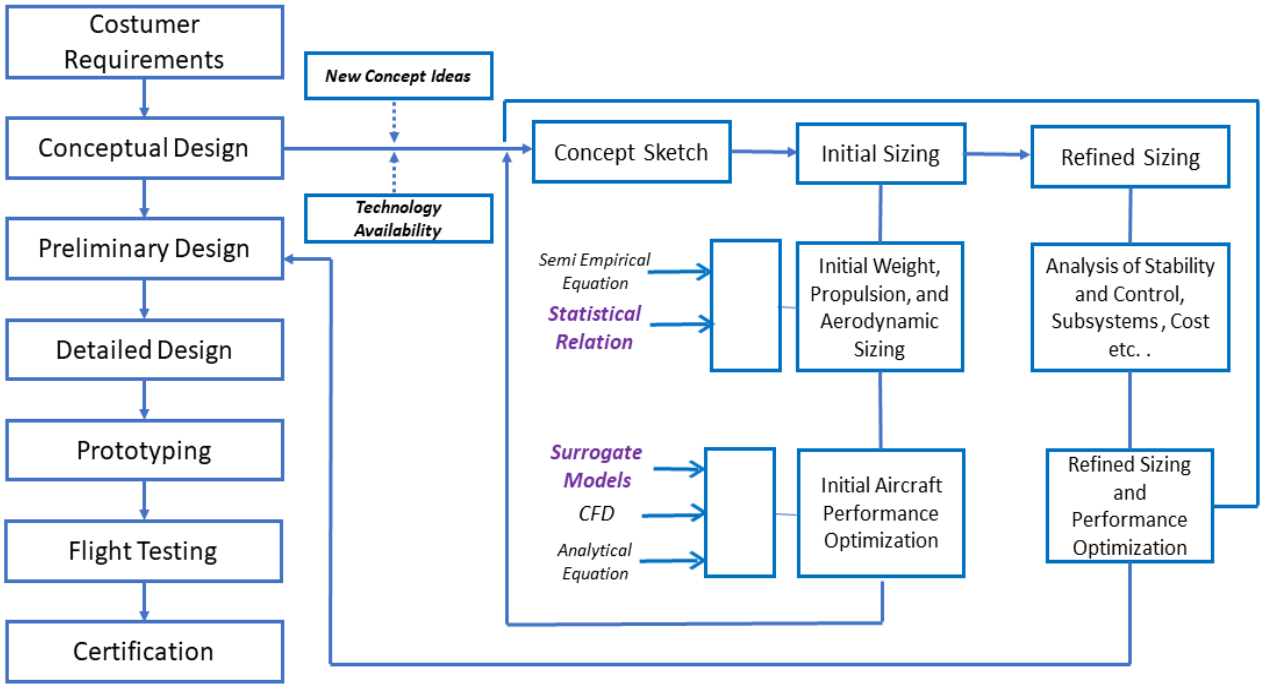

Figure 1-2: Research Contribution

``

CHAPTER 2: **LITERATURE REVIEW**

Statistical techniques are widely used in aircraft/rotorcraft design, particularly during the preliminary design phase, because at this point, rapid assessment of the design is more crucial than analysis fidelity [7]. Therefore, aircraft/rotorcraft design software is specially equipped with statistical-based sizing modules that estimate aircraft/rotorcraft geometric, weight, and performance parameters from the mission profile. These results are then helpful in detailed design and analysis.

Design trends are a principal component of aircraft/rotorcraft design software and are widely used in the conceptual design phase. These trends and other semi-empirical rules help design engineers develop suitable working point configurations, thereby circumventing cumbersome comprehensive analysis during the early design phase. Moreover, they show some physical constraints that may not be known at an earlier stage but should be considered to devise a flyable configuration [8].

In the rotorcraft domain, design trends were broadly explored by Rand and Khromov [8]. The study aimed to develop a set of empirical equations for sizing rotorcraft geometric parameters and estimating power and flight performance parameters during the preliminary design phase. For this purpose, the database of more than 180 rotorcraft was utilized to develop several linear/non-linear and multiple linear regression models among rotorcraft weight, geometric, engine, and performance parameters. Similarly, Lier [9] investigated statistical methods for rotorcraft preliminary sizing and design. A database of about 80 rotorcraft was analyzed to identify highly correlated design trends. The study concluded that the mass properties of rotorcraft are highly correlated with its physical dimensions, such as main rotor diameter, overall height, fuselage length, etc. In contrast, performance parameters like speed and range show a weak correlation with all the other design variables in the dataset.

Scaling laws in nature are demonstrated in an interesting study conducted by Sullivan *et al. [10]*. The study investigated avian scaling laws and discovered that the tensile strength of wing-humerus bone is the limiting factor that dictates a bird's mass such that humerus bone length and feather length vary proportionally to the bird's mass raised to the power 0.33 and 0.44, respectively.

``

The primary goal of conceptual design is to determine candidate designs' overall shape, size, weight, and performance parameters. In this regard, design trends obtained from pre-existing flying configurations prove valuable, especially for preliminary sizing. The sizing task determines the geometric dimensions, power, and weight estimation of aircraft/rotorcraft to perform a specified set of design conditions and mission requirements. Design trends used in preliminary sizing in both aircraft and rotorcraft domains [11-15] and the potential research gaps are summarized in fig. 2.1 and fig. 2.2 respectively.

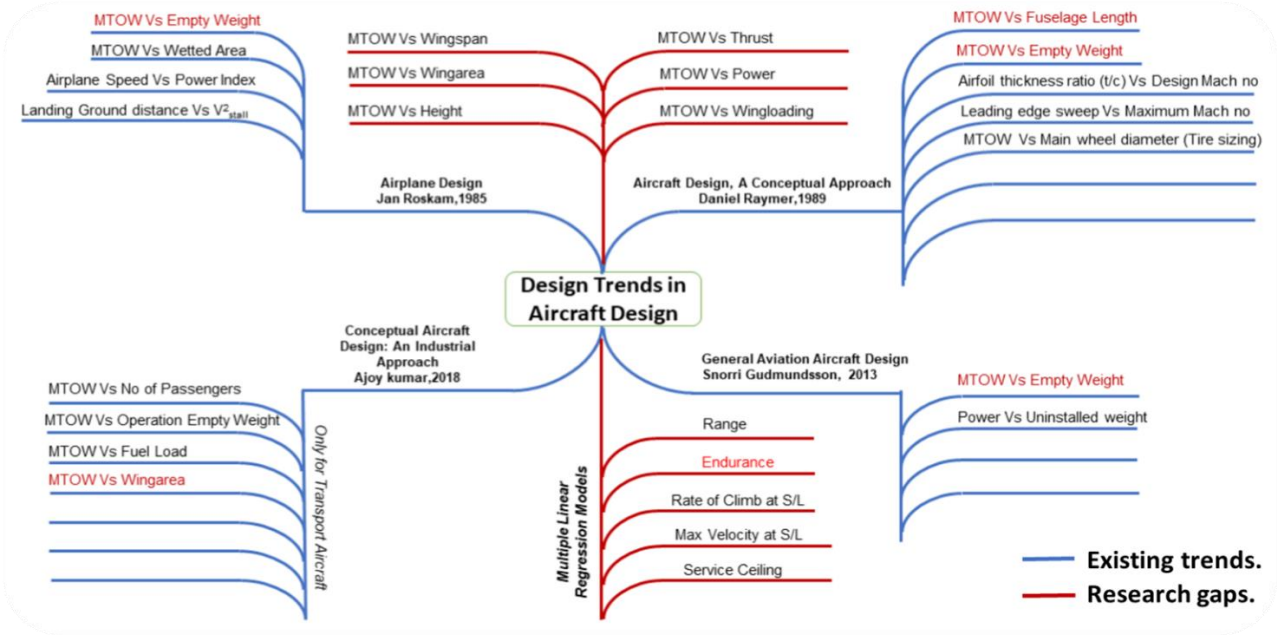

Figure 2-1: Research Gap (Aircrafts)

``

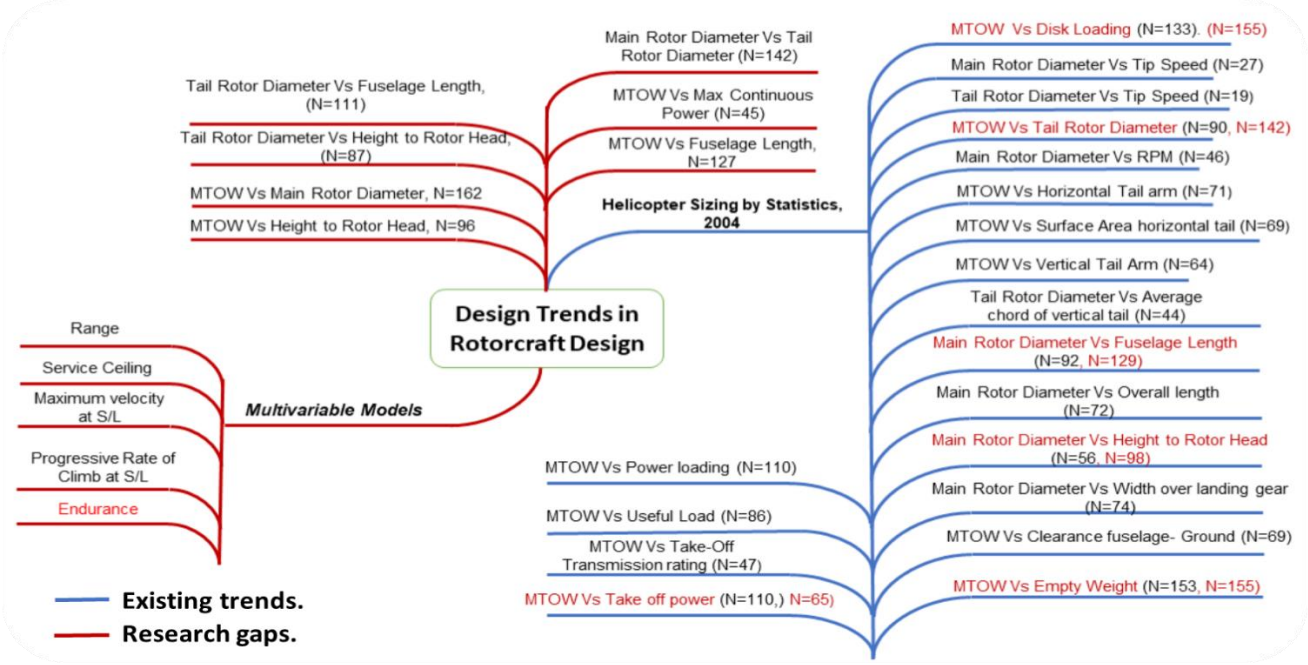

Figure 2-2: Research Gap (Rotorcrafts)

Surrogate modeling is used in various fields for many diverse applications, especially its contribution to the engineering domain is commendable. These models have enabled engineers to tailor current practices and develop efficient designs, saving time, effort, and money. To benefit the existing system, surrogate models can predominantly be used in two ways:

Design Estimation: To estimate the outcome by constructing efficient models that reduce computational time and cost and serve as a simple alternative to existing methods. These models come in handy, particularly during the initial design phase.

Design optimization: Surrogate models are used to find global or local optima quickly [16]. It serves as a swift and straightforward alternative to conventional optimization methods which are based on time exhaustive analysis codes. However, it is to be noted that surrogate-based optimization is only an approximation to the true optimum. That is why these surrogate models need to be updated regularly with the inclusion of new sample points.In addition to that, the surrogate models help to gain deeper insight into functional variables of design space. It allows engineers to identify variables that have a more significant impact, thus focusing on more critical variables. Such understanding may often be derived from the equations resulting from surrogate construction.

ZH Han and KS Zhang conducted a detailed study on different surrogate techniques [17]. Their research examined the response surface method (RSM), kriging, and radial base function (RBF).

``

RSM is a polynomial approximation model in which the least square regression technique fits the sampled data while kriging is an interpolation of observed data. In contrast, RBF is an alternative interpolating technique whose value depends on the distance from the origin. The research concluded that quadratic response surface models (RSM) are well suited for local optimization problems with relatively smaller design space. On the other hand, Kriging and RBF give better results for global optimization problems with relatively complicated design space and multi-modal and highly nonlinear functions.

Multiple linear regression was used by the "Aviation research laboratory" of the University of Illinois in an unclassified report related to "predictor display for aircraft simulators" [18]. The predictor display system predicts the aircraft's position and orientation in the future. The standard method for obtaining the predictor information is to use a complete, fast-time model of the controlled vehicle. Quite an alternative to the pre-existing standard model statistical approach based on the least square method is utilized to predict six degrees of freedom of an aircraft. The results concluded that the regression approach gives a more accurate prediction equation, and thus, it is a more feasible alternative to complete fast time models.

Similarly, Ghasmi Hamid [19] carried out a comparative analysis on regression techniques and point-mass models to predict aircraft trajectory. A dataset was obtained from two months of radar and meteorological recording, after which principal component analysis (PCA) was carried out to reduce the problem's dimensionality. The research concluded that regression methods perform better than the point-mass model.

Similarly, Othman and Kanzaki [20] carried out an interesting study to develop surrogate models for aerodynamics. The proposed aerodynamic surrogate models developed using the Kriging approach have been identified as an efficient tool to complement high fidelity solvers.

A recent study on design trends and surrogate modeling is carried out by two NUST graduates Adnan Ashraf and M.Tashfeen., A.Ashraf [21] has surveyed UAVs. He explored design trends and surrogate models for UAVs. Similarly, M.Tashfeen [22] has extended the concept to encompass fixed-wing aircraft. Their findings are applaudable. Indeed, much of the current research stands on their established methodology. Both the researchers have developed regression models that are generalized for all aircraft categories. However, aircraft are designed for a specific mission profile; therefore, design trends within one aircraft category cannot be applied to another.

``

Some of the shortcomings identified in their study are mentioned below.

I. Propulsion parameters, i.e., thrust/ power, are arguably the two most significant parameters that dictate aircraft performance, esp., “Rate of climb” and “Max velocity at S/L”. Contrary to the fundamentals of aeronautics, these parameters are seen missing in surrogate models of UAVs.

II. The prediction ability of models is not mentioned; therefore, the model’s accuracy to unseen data is unknown.

III. Though some of the design trends identified in both studies are statistically significant and strongly correlated, they are trivial in aircraft design. However, in this research, all probable simple relations were passed through three-filters specifically designed to handpick only those statistically significant, strongly correlated, and significant from aircraft/rotorcrafts design perspective.

Before starting the current study, a detailed analysis of the previous research was conducted, and all the weaknesses as mentioned earlier were duly addressed.

``

CHAPTER 3: **METHODOLOGY AND PROBLEM FORMULATION**

The adopted methodology is delineated in this chapter. It explains the sources and type of data and the statistical tools used during the process. Furthermore, statistical parameters used to determine the accuracy of the models are briefly explained subsequently. MATLAB® is utilized in single variable model building and Minitab® V19 for multivariable modeling. There are different techniques to build surrogate models; however, after scrutiny and studying the parameters' behaviors, scalable relations were made using power laws, and multiple linear regression (MLR) techniques are used in multivariable modeling.

3.1 Data Collection and Interpretation

Aircraft data was compiled from "Janes All the world aircraft" [23], rotorcrafts data from "Jane's Helicopter Markets and Systems" [24], and birds data is collected from "Flight characteristics of birds" [25].

Based on aircraft type and its mission profile specified in ref 17, aircraft are broadly categorized into ten groups discussed in Table 3.1.

S/No	Category	Count
1	Utility aircraft	360
2	Agricultural planes	16
3	Sport-planes and Aerobatics	33
4	Amphibious planes	18
5	Motor-glider	17
6	Fighters	23
7	Trainer	27
8	Transport aircraft	54
9	Business jets	60
10	Freighters	18
Total		**626**

Table 3.1: Aircraft Database Summary.

The collected parameters were classified into geometric, weight, engine, and performance parameters for each aircraft, as shown in Table 2. In addition to that, geometric parameters are

``

pictorially presented in figure 2 as well. The wing area, defined in Jane's literature, is taken as the

total projected area of a clean wing (no projecting flaps/slats and so on), including all control surfaces and fuselage area bounded by leading and trailing edges projected to the centerline. The length of the aircraft is taken from the nose of the aircraft to the aft-most geometric point along the longitudinal axis. The geometric wingspan is from tip to tip, including wingtips, and for the fighters, it is the wingspan over missiles. The aircraft's height is from the ground with deployed landing gears (if any) up to the vertical tail. The maximum take-off weight excludes taxi fuel. Reference power values are mentioned at full take-off power with engines installed at sea level. Similarly, thrust is referenced as the maximum available installed engine thrust at sea level for jet configurations.

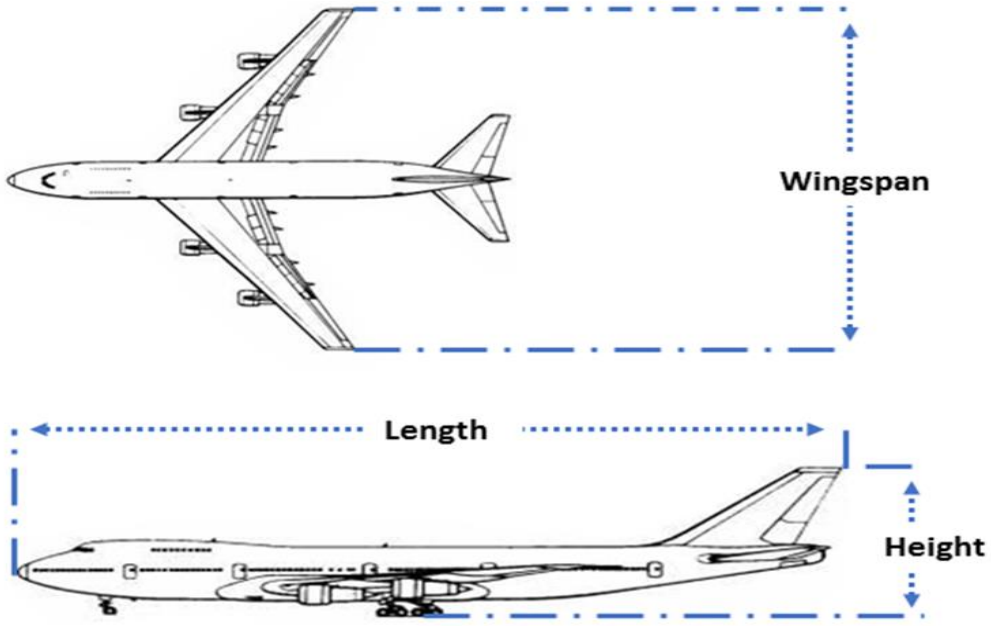

Figure 3-1: Pictorial representation of aircraft geometric parameters.

Aircraft performance parameters include range, maximum rate of climb at sea level, maximum velocity at sea level, and service ceiling. The range available for airliners is at design load and correct atmospheric conditions. However, in the case of fighter aircraft, the ferry range is the maximum range that an airplane can fly with maximum fuel load, optionally with extra fuel tanks and minimum equipment. Maximum velocity and Maximum rate of climb are at sea level

``

conditions. It should be noted that not all geometric, design, and performance parameters are collected due to the non-availability of one or the other in literature.

Geometric Parameters	Weight Parameters	Propulsion Parameters	Performance Parameters
Aircraft Length (m)	MTOW (kg)	Thrust (kN)	Range (km)
Wingspan (m)			Rate of Climb at S/L (m/s)
Wing area (m^2)	Empty weight (kg)	Power (kW)	Vmax at S/L (km/hr)
Aircraft Height (m)			Cruise Velocity (km/hr)
			Service Ceiling (m)

Table 3.2: Aircraft Design and performance parameters considered in the study.

3.2 Rotorcraft Classification

As defined by ICAO, rotorcraft are "supported in flight by the reactions of the air on one or more rotors. A rotorcraft or rotary-wing aircraft is thus a heavier-than-air flying machine that uses rotors for lift generation and steering. Generally, rotorcraft is equipped with a main rotor and tail rotor. The main rotor is responsible for lift generation while the tail rotor counters the torque produced by the main rotor. Based on torque counteracting mechanism, rotorcraft are primarily divided into four main class details, summarized in fig 3.2.

``

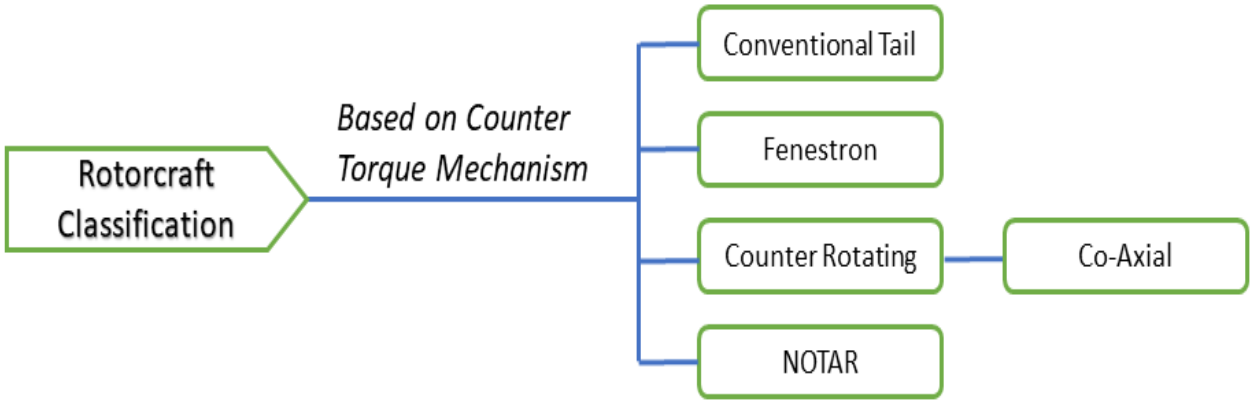

Figure 3-2: Rotorcraft classification based on antitorque mechanism.

Conventional tail rotors: It is the most common configuration in which a rotorcraft has one main and one tail rotor. The Main rotor is responsible for generating lift, propulsive force for flight, and necessary forces and moments to control the position and altitude of a rotorcraft. In contrast, the tail rotor counteracts the torque and provides the essential yaw control. Apart from the weight advantage due to its more straightforward design, conventional tail rotors require relatively less power, produce reasonable yaw control, thus contributing significantly to yaw damping and directional stability in forward flight [26]. However, free tail rotors generate more noise, are potentially dangerous to ground personnel, and are more prone to structural failure when swung into foreign objects.

Fenestron: Fenestron, also known as a fan in tail or fan in fin, is a tail rotor configuration in which the tail rotor is integrally housed in the tail boom and operates more like a ducted fan. It was first designed in 1943 by British aeronautical engineer C.G Pullin. The concept was meticulously refined over more than two decades, and finally, the Sud Aviation SA-340 became the first rotorcraft to put the idea into the skies [27]. Furthermore, unlike conventional tail rotors, which typically have two, three, or maximum of four blades, Fenestron rotors have more blades ranging from 8 to 13. Some of the key advantages and critical challenges of using the Fenestron configuration are summarized below.

Key Advantages:

``

i. The shroud protects the tail rotor, making it less susceptible to colliding with foreign objects. Additionally, the enclosed tail is safer for ground crew working near the helicopter during takeoff and landing.
ii. It reduces pilot workload and improves anti-torque efficiency.
iii. Fenestron configuration is quieter compared to conventional tail rotor [28].
iv. It requires less power during the cruise phase [29].

Critical Challenges

i. The enclosure adds weight and drag penalty [30].
ii. It requires more power during the hover phase [29].
iii. It is a complex design compared to conventional tail rotors, which means higher manufacturing and production costs.

NOTAR: To reduce noise and eliminate safety-related issues associated with tail rotor, McDonnell Douglas Helicopter Systems (through their acquisition of Hughes Helicopters) under Army/DARPA contracts developed a unique mechanism that uses jet actuation to counteract the torque generated by the main rotor. The system consists of an enclosed fan, circulation control tail boom, valved turning vane array, and a vertical fin [31], as shown in figure 3.3.

``

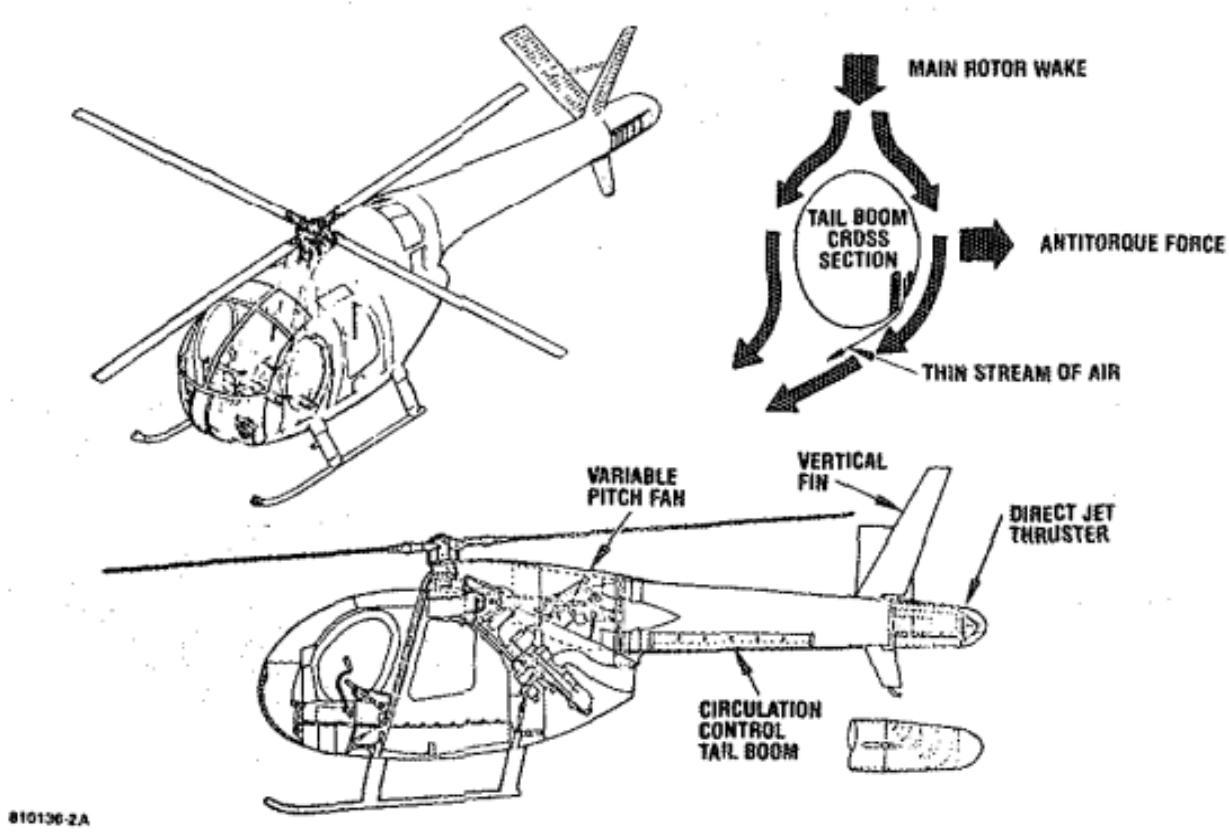

Figure 3-3: Working Principle of NOTAR Configuration.

The variable pitch fan within the tail boom builds a large volume of low-pressure air, which escapes through two slots and creates a boundary layer flow of air along the tail boom using the Coanda effect. The Coanda effect keeps the air efflux attached to the boom surface, thereby inducing the downwash of the main rotor to form a circulating flow. This results in a lateral force acting on the tail boom that compensates for the main rotor torque [32].

Coaxial Counter-Rotating Rotors: In this kind of rotorcraft, both lift generation and torque counteraction are done by a pair of rotors mounted on top of one another on concentric shafts turning on the same axis of rotation but in the opposite direction. Due to the absence of a tail rotor and a significantly shorter tail boom, this configuration is more favorable in confined spaces. In addition to their compact design, these are comparatively quieter, more stable, and have better hover capabilities. However mechanical complexity of the hub is a major drawback of this configuration.

``

Figure 3-4: Four types of Rotorcraft configurations.

The collected parameters for rotorcraft include geometric, weight, propulsion, and performance parameters. Rotorcraft geometric parameters have Main-Rotor diameter, Tail-Rotor diameters, Height to the rotor head, and fuselage length as illustrated in fig 3.5.

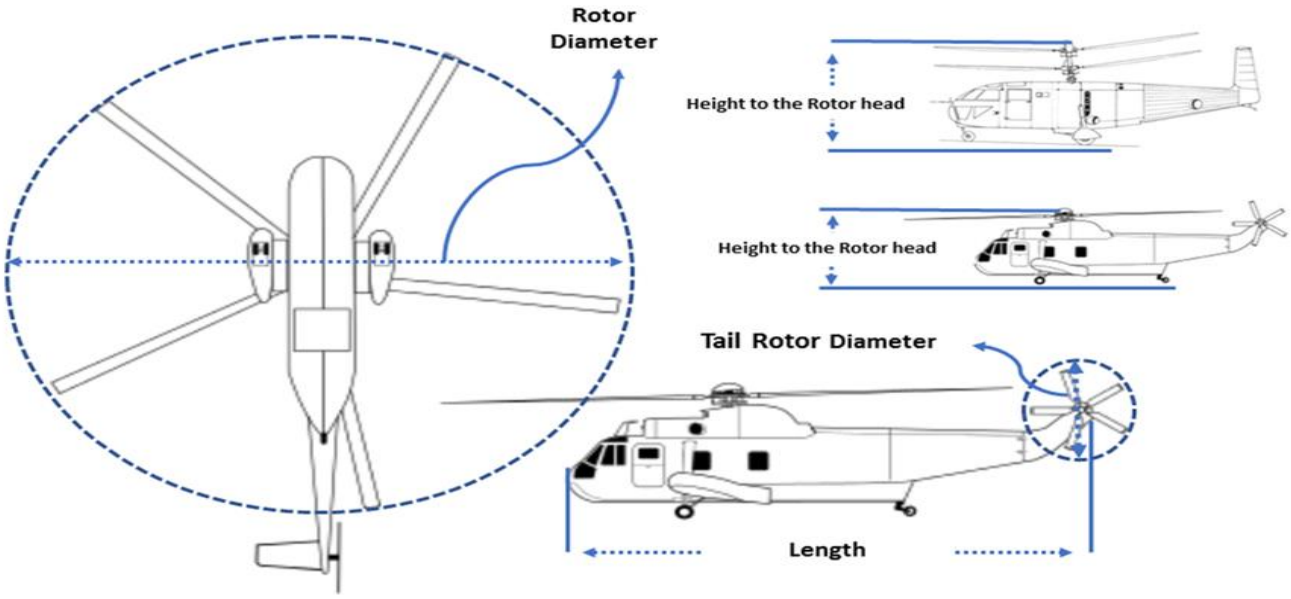

Figure 3-5: Pictorial representation of rotorcraft geometric parameters.

``

MTOW as defined in Jane's helicopter markets and the system is Maximum takeoff with slung loads or maximum internal fuel. The range is at designed load, maximum fuel, economic cruise velocity, and ISA conditions at a certain altitude. The rate of climb and maximum level velocity is at sea level conditions. The design and performance parameters considered in the study are further summarized in Table 3.3.

<table>
<tr><th>Geometric parameters</th><th>Weight parameters</th><th>Propulsion parameters</th><th>Performance variables</th></tr>
<tr><td rowspan="2">Fuselage Length (m)</td><td rowspan="2">MTOW (kg)</td><td rowspan="2">Maximum Continuous Power (kW)</td><td>Range (km)</td></tr>
<tr><td>Endurance (hrs)</td></tr>
<tr><td>Height to the Rotor head (m)</td><td></td><td></td><td>Rate of Climb at S/L (m/s)</td></tr>
<tr><td>Main-Rotor Diameter (m)</td><td rowspan="2">Empty Weight (kg)</td><td rowspan="2">Maximum Takeoff power (kW)</td><td>Vmax (km/hr)</td></tr>
<tr><td>Tail-Rotor Diameter (m)</td><td>Cruise-Velocity (km/hr)</td></tr>
<tr><td></td><td></td><td></td><td>Service Ceiling (m)</td></tr>
</table>

Table 3.3: Rotorcraft design and performance parameters considered in the study.

3.3 Statistical Significance Test and Correlation Analysis

All possible simple relations among all collected design variables specified in table 3.2 and table 3.3 for both aircraft and rotorcraft are passed through three filters.the aim of which is to pick only those relations which are statistically significant, strongly correlated, and non-trivial from an aircraft/rotorcraft design perspective. The first filter allows only statistically significant relations to pass on; the second filter is based on Spearman's correlation coefficient "ρ," which enables us to pick strongly correlated relations. The last filter is based on theoretical knowledge of aircraft/rotorcraft design. It allows us to extract those design trends that have substantial utilization in the aircraft/rotorcraft conceptual design phase. After implementing three filters, it was found that aircraft geometric and engine parameters were strongly correlated with maximum takeoff weight. Therefore, MTOW is used as a primary independent variable in single variable modeling.

The three filter test adopted to develop single and multivariable models is further summarized in figure 3.6.

``

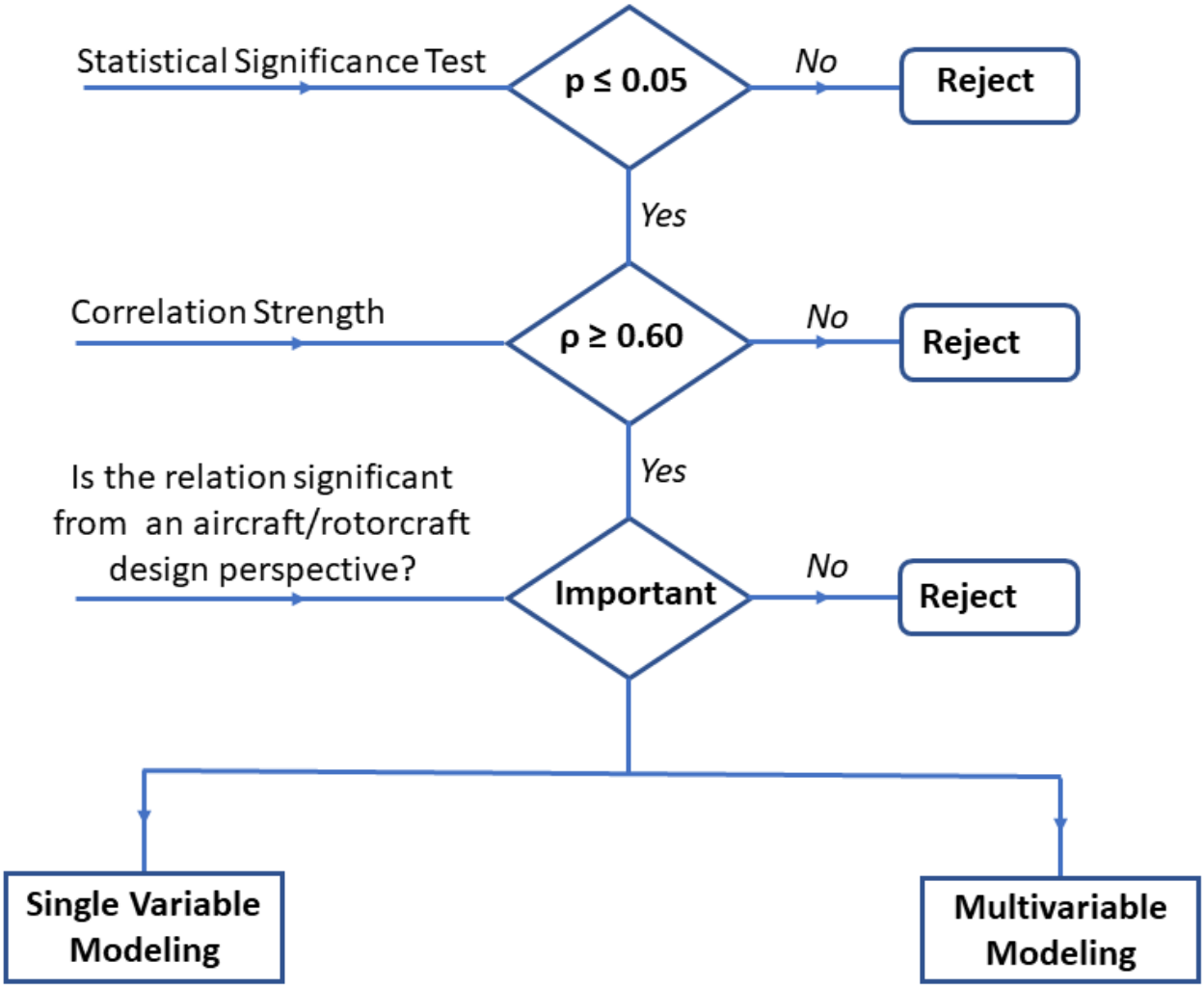

Figure 3-6: Selection methodology for single variable modeling.

The two most fundamental questions about any proposed relation are:

I. What is the probability that the relationship between any two variables is entirely coincidental?

II. If the relationship is not just random chance, what is the strength of a relationship?

The significance test addresses the first question, which rules out the probability of random occurrence of any relationship. This analysis uses a p-value of 0.05, meaning relations with a $p > 0.05$ are removed from the study.

``

To address the second question, correlation analysis has been carried out, which evaluates the strength of the relationship between two variables. A Correlation matrix is a valuable statistical tool to determine the strength of correlation among all variables in a large dataset. The Pearson correlation coefficient is one of the most commonly used parameters to quantify the linear association between two variables. Its value ranges from -1 to +1. A value of -1 and +1 implies positive and negative linear relationships, while 0 means no linear relationship between any two variables. Since the Pearson correlation coefficient only accounts for linear relationships. The Spearman correlation rank coefficient is used in this research because it accounts for both linear and non-linear monotonic relationships between either two discrete or continuous variables. Spearman rank's correlation coefficient for untied ranks is given by:

$$\rho = 1 - \frac{6\Sigma\, d_i^2}{n(n^2-1)} \tag{1}$$

where n is no of cases, and di is the difference between the two ranks of each observation
Spearman rank's correlation for tied ranks:

$$\rho = \frac{\Sigma_i(x_i-\bar{x})(yi-\bar{y})}{\sqrt{\Sigma_i(x_i-\bar{x})^2\Sigma_i(yi-\bar{y})^2}} \tag{2}$$

Its value also varies from -1 to +1, where -1 and +1 indicate a strong negative and positive relationship, respectively, while 0 suggests no association between the two variables.
A spearman rho coefficient greater than 0.40 indicates strong relationships, 0.30-0.39 indicates moderate relationships, and less than 0.20 indicates poor relationships [33].

3.4 **Single Variable Modeling using Power Law**

The power law is used to find one to one relationship between any two variables. Using "Y" as a dependent variable and "X" as an independent variable, the power-law scaling is:

$$Y=\alpha*X\hat{}\beta$$

where α is the normalization constant and β is the power of the independent variable. The β value in the power-law gives an essential insight into the relation such that for the β>1, the relation is superlinear, β=1 means linear, and β<1 means sublinear. This means the β value determines whether the dependent variable increase radically or normally.

``

Different equations (i.e., Fourier, polynomial, exponential, Gaussian, and power-law) were applied to a given data set to form scalable relations among aircraft parameters. It was found out that only the power-law equation best fits the data set.

3.5 **Multivariable Modeling**

Multiple linear regression (MLR) is a statistical technique often used in multivariable modeling to predict a response variable's outcome by combining several explanatory variables. It is the extension of simple linear regression because it involves more than one explanatory variable.

It is given by:

$$y = \beta_0 + \beta_1 x_{i1} + \beta_2 x_{i2} + \cdots \ldots . \beta_p xip + \varepsilon$$

where "*y*" is the dependent (response) variable, β_0 is the intercept (mean of the dependent variable when all explanatory variables are zero), β_p is the slope (change in *y* w.r.t *x*), $\beta_0 \ldots . \beta_p$ are called regression coefficients, and ε (Random part) explains the variability of response about the mean [34]

Various diagnostics checks, such as Mean absolute percentage error (MAPE), Maximum error, Minimum error, R-square, Adjusted R-square, R-predicted, t-test, and f-test, were used to assess the accuracy of the built model(s) and their resulting estimate. Moreover, some additional tests were carried out to ensure that the data set meet all the necessary assumptions of Multiple linear Regression, which include (but are not limited to) the Anderson darling test for normality, the variance inflation factor "VIF" for multicollinearity, and so on.

R^2, also known as the coefficient of determination, measures the amount of variability in the response variable explained by the predictor variable(s) in the regression model. It is a statistical test used in the perspective of statistical models to either predict future consequences or the testing of hypotheses based on the related information. Its value ranges from 0 to 1, and it is calculated using;

$$R^2 = 1 - \frac{SS_{res}}{SS_{tot}}$$

where the sum of Square of residuals (SS_{res}) is given by;

``

$$SS_{res} = \sum_i (y_i - f_i)^2$$

and the total Sum of Squares (SS_{tot}) by:

$$SS_{tot} = \sum_i (y_i - \bar{y})^2$$

Adjusted R-squared is a modified version of R-squared adjusted for the number of predictors in the model. It increases only if the new term improves the model more than expected by chance; otherwise, it decreases if the new predictor-term enhances the model by less than expected by chance. The adjusted R^2 is more critical when the model contains more than one independent variable. It is given by:

$$R^2_{Adjusted} = 1 - \frac{(1 - R^2)(N - 1)}{N - p - 1}$$

where "R^2" is the sample R squared value, "p" is the number of predictors, and "N" is the total sample size. $\mathbf{R^2_{predicted}}$ is used to assess the model accuracy for the unseen data. It is calculated by systematically removing each observation from the data set, evaluating a new regression model, and determining how accurately it predicts the removed observation [35].

Mean absolute percentage error abbreviated as MAPE, is a statistical measure to determine the accuracy of the forecast system. It measures the accuracy in the form of a percentage.

$$\text{MAPE} = \frac{1}{n} \sum_{i=1}^{n} \left| \frac{y_{icalculated} - y_{iobserved}}{y_{iobserved}} \right| \times 100$$

MAPE is easy to interpret, robust to outliers; however, it is undefined for the data points where the value is 0 and biased towards predictions that are systematically less than the actual values.

In addition, maximum and minimum errors are the maximum percentage error and the minimum percentage error in the dataset, respectively. Moreover, the maximum error is instrumental in identifying the unique/ off-design aircraft configurations.

$$Maximum\ Error = \text{Max} \left| \frac{y_{icalculated} - y_{iobserved}}{y_{iobserved}} \right| \times 100$$

$$Minimum\ Error = \text{Min} \left| \frac{y_{icalculated} - y_{iobserved}}{y_{iobserved}} \right| \times 100$$

``

Under the null hypothesis, the t-test is a hypothesis test in which test statistics follow a t-distribution. It is used to determine whether two sets of data are substantially different from one another. It is most frequently applied when the test statistics follow a normal distribution and the value of the scaling term is known. If the scaling term is unknown, it is substituted by an estimate based on the given data. It is used to assess the significance of the individual regression coefficients.

The t value is calculated by:

$$t = \frac{M_x - M_y}{\sqrt{\frac{S_x^2}{n_x} + \frac{S_y^2}{n_y}}}$$

$$S^2 = \frac{\sum(x - M)^2}{n - 1}$$

where *M* is mean, *n* is the number of scores per group, and *x* is the individual score.

F-test is a statistical test in which the test statistic has an F-distribution under the null hypothesis. It is most commonly used when comparing statistical models that have been fitted to a data set to determine which model better fits the population from which the data is sampled. In linear regression F-test tells whether any of the independent variables in a multiple linear regression model is significant or not. It is used to assess the overall adequacy of the model. F value is stated as the ratio of variances of two observations. The association between the variance of two data sets can lead to many estimates.

It is given by:

$$F_{value} = \frac{\sigma_1^2}{\sigma_2^2}$$

where σ^2 is the variance and given by:

$$\sigma^2 = \frac{\sum(x - \bar{x})^2}{n - 1}$$

where "x" is the given value, "$\bar{x}$" is the mean value, and "n" is the total number of tests.

The aircraft database is first split into two groups based on the propulsion system used (jet-driven and propeller-driven). Log transformation is applied to normalize skewed data sets.

``

Multiple linear regression using the least square method is then invoked to develop a surrogate model for aircraft performance parameters.

A least-square method is a standard approach in regression analysis that determines the best line of fit for collecting data. Moreover, stepwise regression is a regression fitting process where an automated procedure occurs in selecting predictive variables.

There are main strategies of stepwise regression: forward selection, backward elimination, and bi-directional elimination.

Forward selection begins with an empty model, adds each explanatory variable one by one, tests the model against the pre-specified criterion, and keeps the most statistically significant variables, repeating the procedure until the results are optimal. Whereas backward elimination starts with a model that contains all potential explanatory variables, deletes one at a time, then tests the model to see whether a removed variable is statistically significant. Bi-directional elimination is a combination of forwarding selection and backward elimination. It starts with an empty model then adds or removes each potential term to make a new model. As with forwarding selection, the procedure begins with an empty model then adds each candidate variable using a pre-specified criterion at every step; the procedure also considers the statistical consequences of dropping variables previously included. So, In bi-directional elimination, it is quite possible that the variable added in Step 2 might be dropped in Step 4 and added again in the final step. In this analysis, bi-directional elimination is used.

``

CHAPTER 4: **RESULTS AND DISCUSSION**

4.1 Aircraft Design Trend Using Power.

All aircraft look alike in terms of wings, fuselage, and other notable features, but they all vary in size. When we compare two aircraft, one of which is twice as heavy as the other, we notice that it is not just the weight that has increased; the aircraft also needs bigger wings and other geometric changes to make it fly-worthy. In this regard, scalable relations among aircraft parameters show how thrust/power and other geometric parameters such as aircraft length, aircraft height, wing-area, wing-span vary with maximum takeoff weight. Furthermore, it provides a clear picture of the one-to-one relationship among aircraft design parameters. This scalability study lays the groundwork for the development of surrogate models for aircraft performance parameters.

Maximum Takeoff Weight is observed to be strongly associated with aircraft geometric and propulsion parameters. In addition to that, MTOW is more often used as the complete figure of merit since it is directly or indirectly related to aircraft operational, performance, and economic properties; therefore, in exploring the design trends for aircraft, MTOW is used as a primary independent variable as shown in table 4.1.

Power Law: $Y = \alpha \times X^{\beta}$								
Predictor (X): MTOW								
S.No	**Response (Y)**	**α**	**β**	**N**	**R-Sq**	**MAPE**	**Max.E**	**Min.E**
1	**Aircraft Length (m)**	0.5025	0.3847	598	0.970	10.70	62.90	0.010
2	**Empty Weight (kg)**	1.522	0.9108	491	0.996	32.10	72.03	0.042
3	**Wingspan (m)**	1.131	0.3132	569	0.951	13.80	63.57	0.019
4	**Wingarea (m^2)**	0.0271	0.7675	485	0.966	48.49	78.13	0.265
5	**Height (m)**	0.2167	0.3524	543	0.961	13.18	56.35	0.080
6	**Thrust (kN)**	0.0175	0.8525	123	0.972	20.57	68.93	0.071
7	**Power (kW)**	0.0027	1.196	461	0.993	23.60	67.94	0.024

Table 4.1: Aircraft Scaling laws

``

I. MTOW Vs Aircraft Length

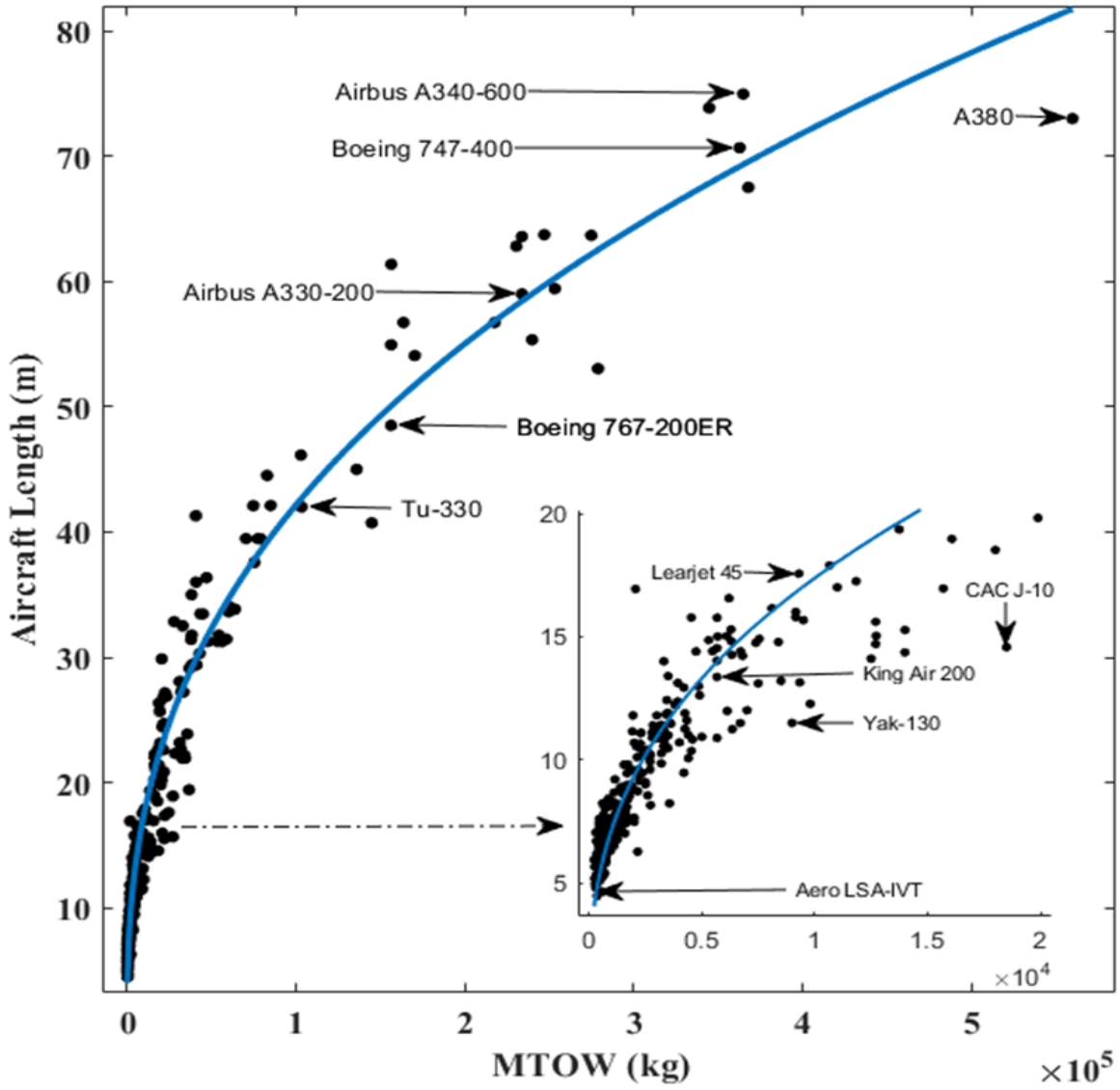

Figure 4-1: MTOW relation with aircraft length.

The trendline between MTOW and aircraft length is sublinear with β value 0.3847. The relationship is close to isometric but not perfectly isometric as anticipated by square/cube law. Square/cube law suggests that "When an object undergoes a proportional increase in size, its new surface area increases to the square of the multiplier and its new volume and mass increase to the cube of the multiplier" [36]. This rapid increase in the mass increases structural stresses, limiting the indefinite increase in the size of the body. Interestingly, aircraft length, aircraft height, and

``

wingspan are all sub-linearly associated with MTOW; all these relations are close to isometric but not perfectly isometric. Perfectly isometric growth would have a volume proportional to a body mass, length proportional to mass raised to the power 1/3, and surface area proportional to mass raised to the power 2/3. The deviation from the perfect isometric growth is due to technological advancements in material strength, which have enabled us to witness aircraft giants like Airbus A380, Airbus Beluga, Boeing 747 and Antonov An-225, etc.

``

II. MTOW Vs Empty Weight

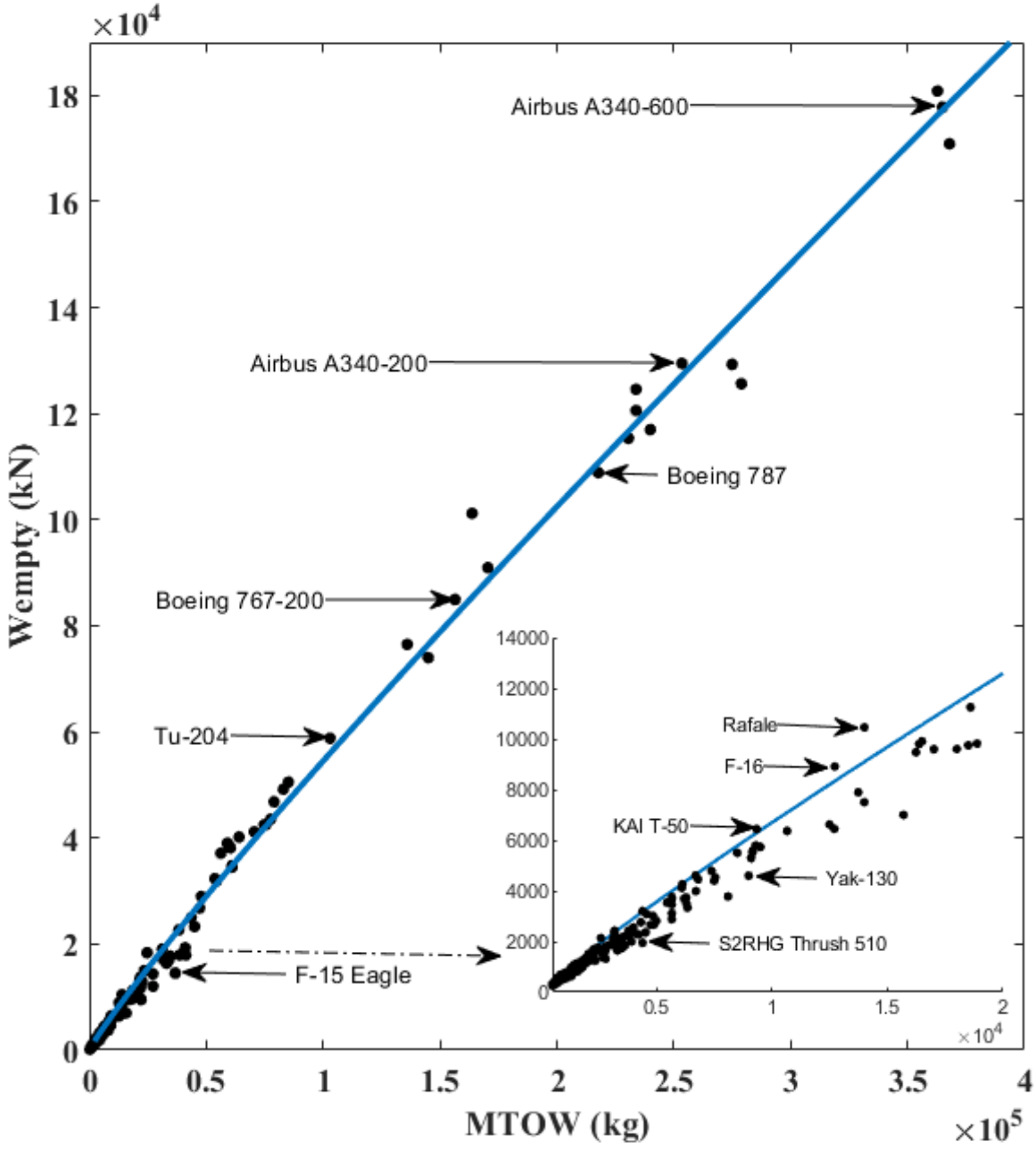

Figure 4-2: MTOW relation with empty weight.

MTOW and empty weight are almost linearly correlated. It has been observed that for the heavy aircraft categories like airliners, freighters, and fighters, empty weight is roughly about 40-50% of the maximum takeoff weight. In contrast, the empty weight of lighter aircraft categories such as aerobatics, amphibious, utility, and motor gliders is approximately 30%-40% of the maximum

``

takeoff weight. Moreover, in the case of agricultural aircraft, empty weight is about 50% of the maximum takeoff weight.

Keeping all other variables intact, aircraft design engineers are more oriented toward reducing empty weight; hence, aircraft that fall below the trendline have a lower empty weight, resulting in increased fuel and payload capacity.

III. MTOW Vs Wingspan

Wingspan and Maximum-takeoff weight are strongly correlated with an R-sq value of 0.95. The trendline is sublinear, rapidly increasing for lighter aircraft, but it flattens out for heavier ones.

Moreover, Fighters, Aerobatics, and Motor-gliders show anomalous behavior in comparison to the overall trendline. This deviation from the overall trendline is due to differences in their design specification following their mission requirement.

Aerodynamics: Fighters operate at higher flight velocities. So, most of their drag is parasitic; therefore, a more extended span requirement to reduce induce drag becomes less significant from a design point of view. In addition to that, low aspect ratio wings are more maneuverable due to their low moment of inertia. This makes low *AR* wings more favorable to fighter aircraft.

Motor gliders, on the other hand, are designed to fly at lower speeds. As a result, a longer wingspan to minimize induced drag is a prominent design feature to consider. High AR wings give better L/D, making the long slender wing more appropriate in motor glider design.

$$CD_i = CD_0 + \frac{CL^2}{\pi e \frac{b^2}{S}}$$

Due to these aforementioned aerodynamic-related reasons, fighter aircraft have a relatively shorter wingspan for a given MTOW, while motor gliders have a longer wingspan than other aircraft categories.

Structure: From a structural perspective, longer wings are more vulnerable to structural failure due to more significant bending stress and torque for a particular load; thus, longer wingspans obstruct fighters from performing high-g maneuvers.

``

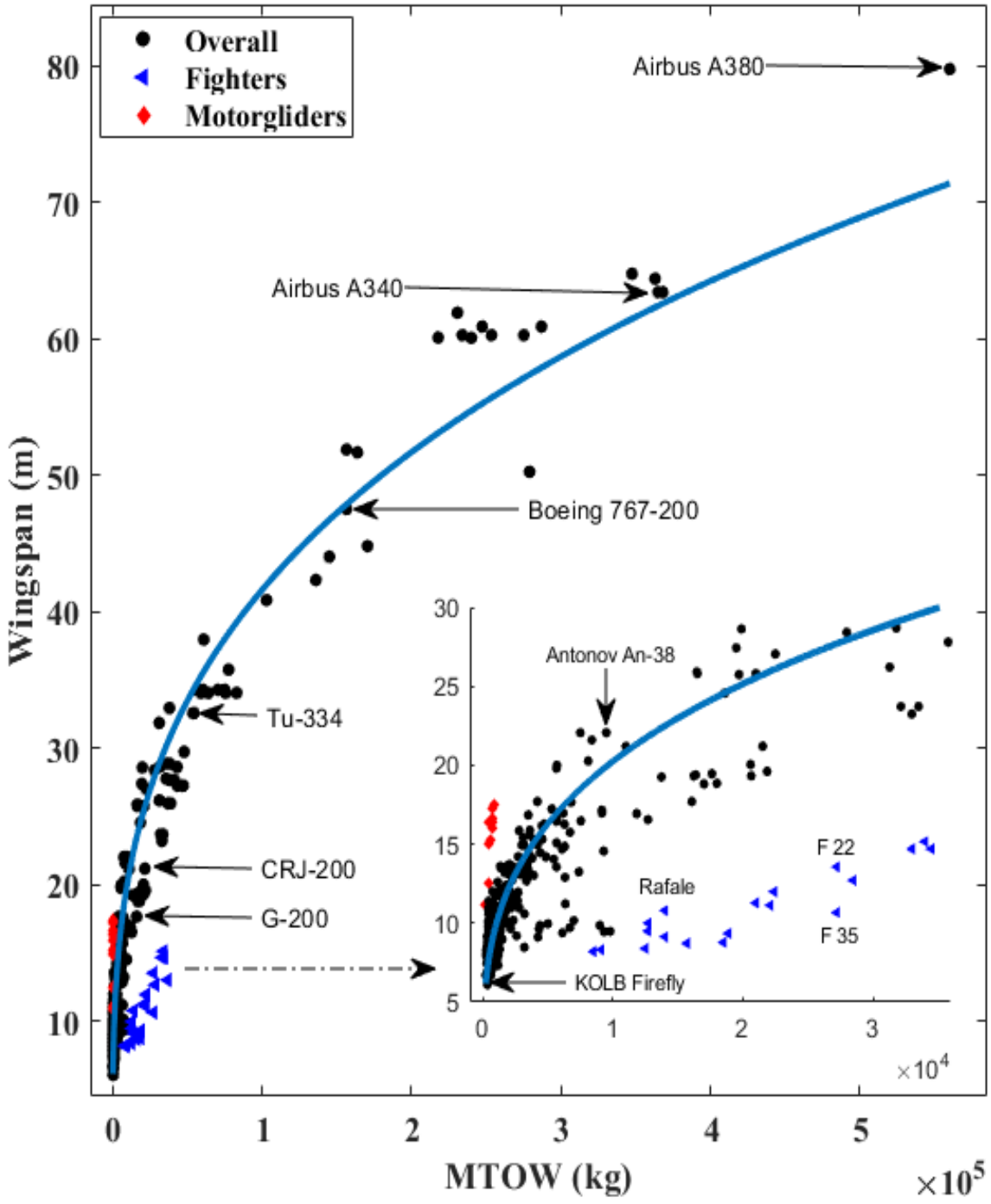

Figure 4-3: MTOW relation with wingspan.

``

IV. MTOW Vs Wingarea

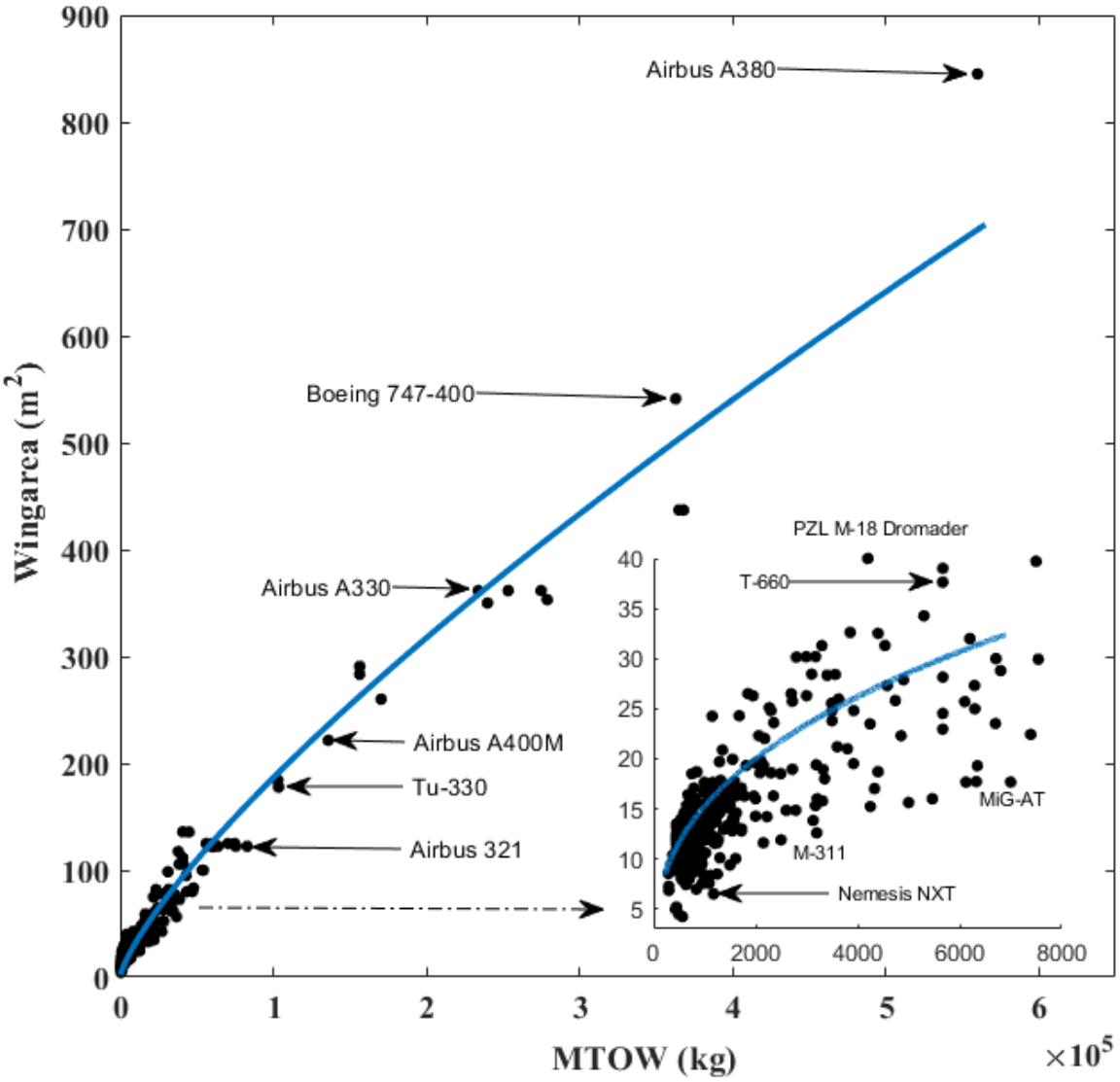

Figure 4-4: MTOW relation with wingarea.

Wing shape, configuration, and size reveal a great deal about an aircraft mission profile: smaller, thinner wings are more favorable for high-speed aircraft like fighters. In contrast, large and high aspect ratio wings are more appropriate for slower aircraft like motor gliders.

Wing area sizing is a critical step in aircraft design. It must be sized to fulfill performance requirements via a matched engine; larger wings perform better at slower speeds, such as landing and takeoff, but have a detrimental effect on cruise performance, the leading segment of the flight envelope. Therefore, wing area sizing is done meticulously to optimize cruise efficiency

``

without losing an aircraft's low-speed field performance. Additionally, there is another conflicting variable: weight penalty; we need a larger wing area to lift a heavier aircraft, but a larger wing increases the aircraft's empty weight.

V. MTOW Vs Aircraft Height

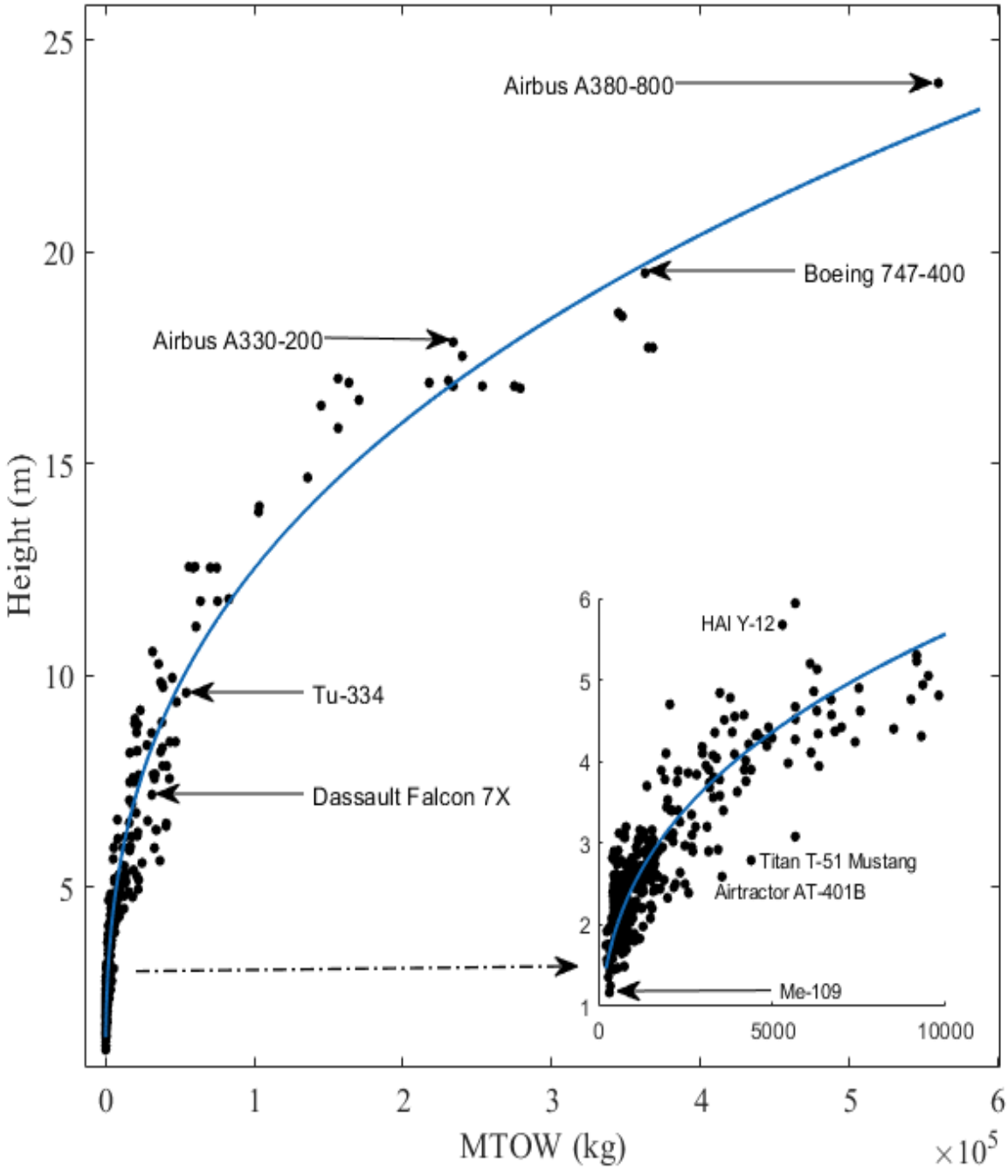

Figure 4-5: MTOW relation with aircraft height.

``

VI. MTOW Vs Thrust/Power Available

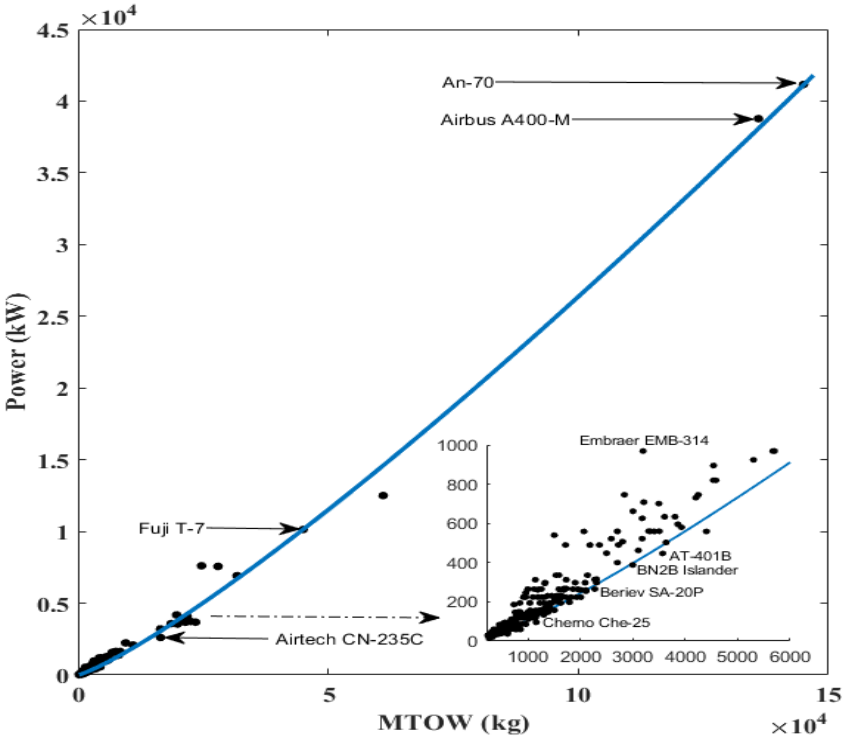

Figure 4-6: MTOW relation with power available.

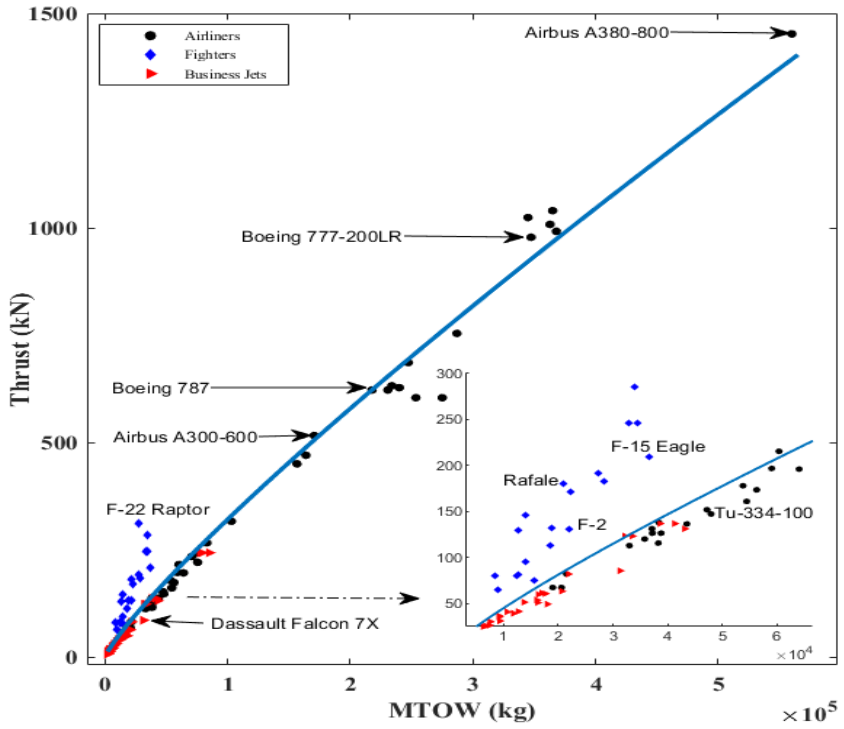

Figure 4-7: MTOW relation with thrust available.

``

MTOW and Power/Thrust are almost linearly correlated; the heavier the aircraft gets, the higher power/thrust required to propel. However, Fighters show deviation from the overall trendline; because combat aircraft are expected to perform high-g maneuvers, short field performances, and quick vertical climbs. That is why for a given MTOW, combat aircraft have higher thrust values than all other aircraft categories.

4.2 Design Trends for Rotorcraft.

Following the application of the three-gate test, only fourteen design trends were chosen for further study out of ninety-one linear models involving fourteen design variables specified in table 3.2. Additionally, the primary independent variables for the selected design trends are carefully selected based on their relevance to overall rotorcraft design.

It is to be noted that the regression equation for conventional tail rotor and Fenestron configuration is only mentioned in subsequent tables. However, the purpose of including NOTAR and coaxial rotors despite their smaller count is to give a reader an idea of where they fit in the rotorcraft family and analyze design trends with respect to each other comparatively.

I. Main Rotor Diameter as a primary independent variable

Main-rotor sizing is arguably the most critical design consideration in rotorcraft design. The primary objective of rotor design is to have the smallest possible rotor that meets the efficiency requirements of the craft. Moroever, the main rotor and the tail rotor are inextricably linked because the former generates torque, which the latter counteracts. Similarly, the size of the main rotor is constrained by the maximum velocity due to compressibility effects at the rotor blade tips.

Design trends in which main rotor diameter is taken as predictor variable are summarized in table 4.2.

Power Law: $Y = \alpha \times X^{\beta}$								
Predictor X: Main Rotor Diameter								
S.No	**Response (Y)**	**Config.**	**α**	**β**	**N**	**R-Sq**	**MAPE**	**Max Error**
1	**Fuselage Length (m)**	**C**	0.8882	1.014	104	0.955	6.54	7.65
		F	0.9065	1.0122	15	0.985	2.75	6.23

``

2	**Height to Rotor Head (m)**	**C**	0.5226	0.7567	81	0.899	6.78	21.02
		F	0.4715	0.8038	8	0.881	3.71	14.74
3	**Tail-Rotor Diameter (m)**	**C**	0.1312	1.127	128	0.928	8.75	35.82
		F	0.1931	0.7058	14	0.709	10.13	34.01

Table 4.2: Main-Rotor diameter as predictor variable in design trends for rotorcraft.

.

``

i. Main Rotor Diameter Vs Fuselage Length

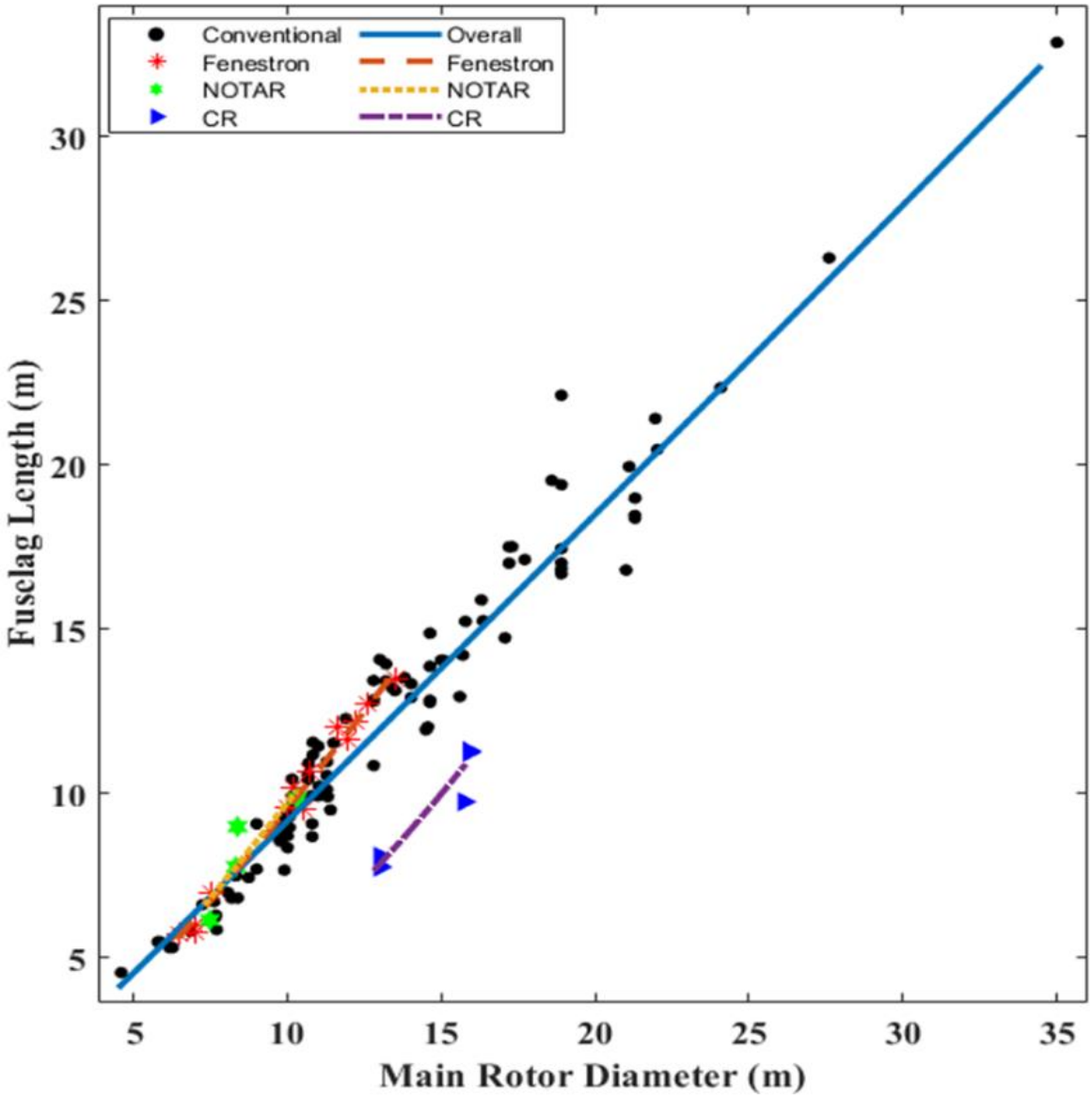

Figure 4-8: Main-rotor diameter relation with fuselage length.

``

ii. Main Rotor Diameter Vs Height to Rotor Head

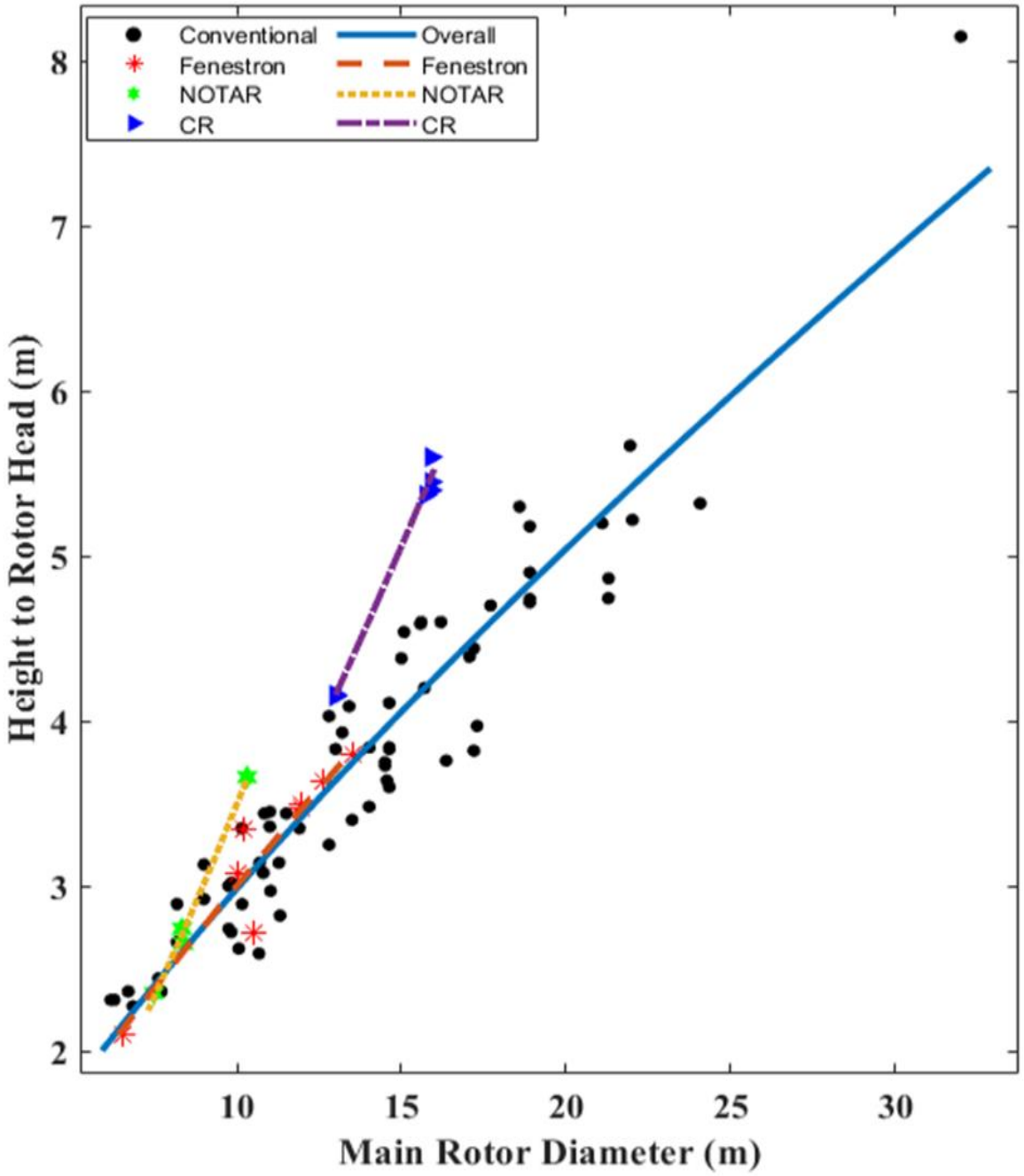

Figure 4-9: Main-rotor diameter relation with height to the rotor head.

‘’Main Rotor Diameter’’ vs. ‘’Height to the rotor head’ is the almost linear trend. However, Counter-Rotating Rotorcraft is the tallest configuration in terms of “height to Main-Rotor head”. C-R rotorcraft are equipped with two overhead rotors to simultaneously produce lift and counter act torque.

``

iii. Main Rotor Diameter Vs Tail Rotor Diameter

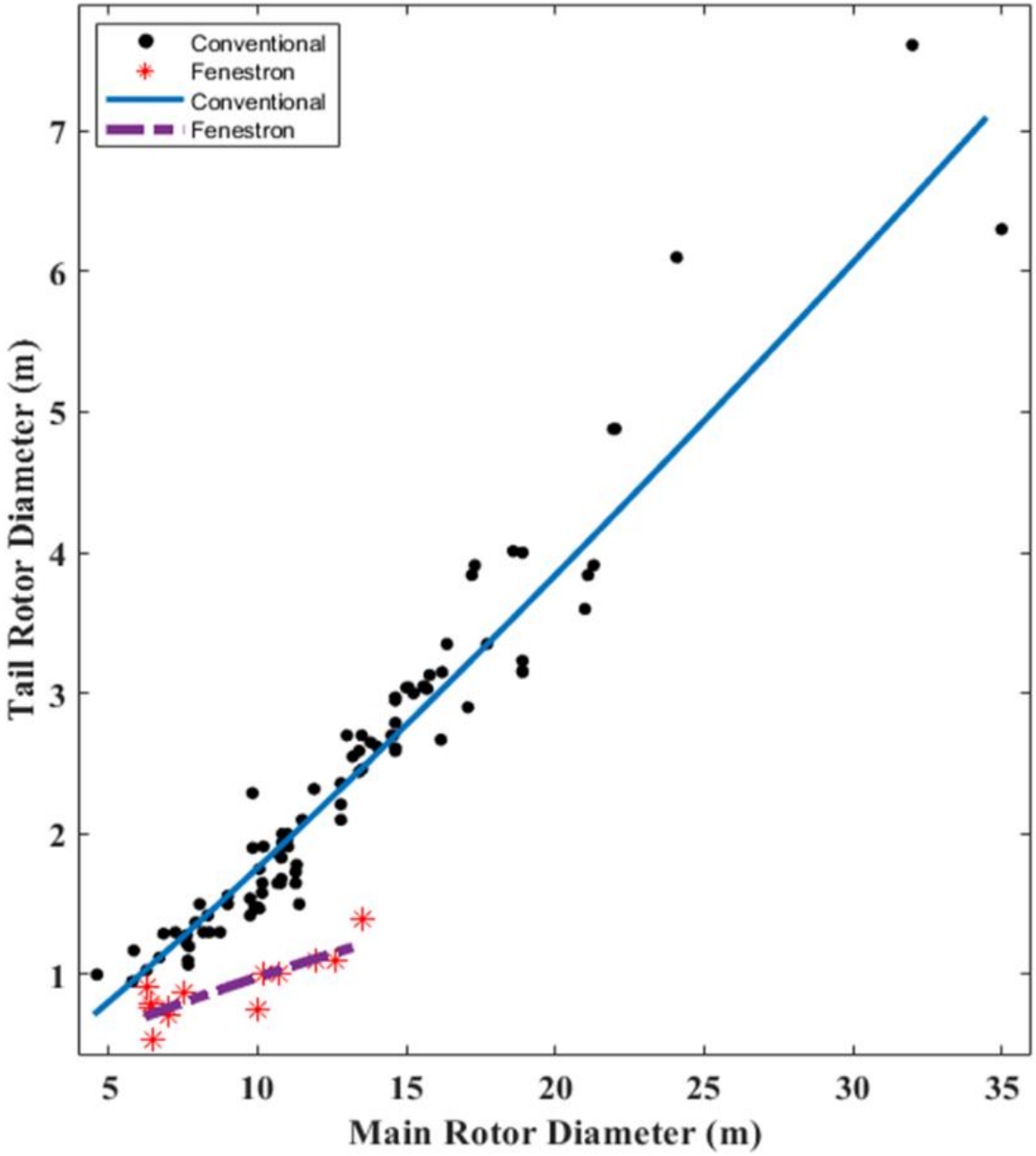

Figure 4-10: Main-rotor diameter relation with tail-rotor diameter.

"Main-Rotor vs. Tail-Rotor' correlation is one of the most significant relation in rotorcraft design. Since they are coupled in their function, their sizing is predominantly dependent on each other. For conventional tail rotorcraft, the trendline is super linear, while it is sublinear for Fenestron configuration. Moreover, the Tail-rotor diameter is approximately (**7.5-15%**) and (**13.25-25%**) of the Main-rotor diameter in Fenestron and conventional tail rotorcraft.

``

Config.	Name	Main-Rotor Diameter (m)	Tail-Rotor Diameter (m)	% Increase
F	Ka-62	13.5	1.4	48.14
C	Mi-54		2.7	
F	Eurocopter EC 135	10.2	1	47.63
C	Aerospatiale SA 318C		1.91	
F	Eurocopter EC 130	10.69	1	46.23
C	Eurocopter AS 350		1.86	
F	Eurocopter EC 120B	10	0.75	49.32
C	Mi-34		1.48	

Table 4.3: Tail rotor comparison of Fenestron and Conventional rotorcraft for the same main rotor diameter.

Fenestron is compact compared to its conventional counterparts. Furthermore, it has been observed that for the same main rotor diameter, tail rotors of conventional rotorcrafts are **45%-50%** larger in size.

II. MTOW as Primary independent variable

As mentioned previously in Section 4.1, MTOW is used as the complete figure of merit because it is directly or indirectly related to aircraft/rotorcraft operation, performance, and economic properties. Additionally, it influences the design of several critical components, such as the rotor, propulsion system, etc. therefore, it is used as a primary independent variable to explore the following design trends.

Design trends with MTOW as a predictor variable are summarized in table 4.4

``

Power Law: $Y = \alpha \times X^{\beta}$								
Predictor X: MTOW								
S.No	**Response (Y)**	**Config.**	**α**	**β**	**N**	**R-Sq**	**MAPE**	**Max.E**
1	Fuselage Length (m)	**C**	0.6795	0.3492	103	0.937	6.63	27.27
		F	0.8686	0.3143	16	0.977	3.68	9.76
2	Empty Weight (kg)	**C**	0.8069	0.9667	127	0.974	11.73	51.84
		F	0.4527	1.022	17	0.979	10.35	54.61
3	Main Rotor Diameter (m)	**C**	0.7661	0.3428	135	0.926	8.47	27.60
		F	1.509	0.2488	17	0.971	3.73	11.57
4	Tail Rotor Diameter (m)	**C**	0.0726	0.4197	126	0.964	7.92	26.29
		F	0.1971	0.2049	16	0.649	12.10	32.98
5	Height to Rotor Head (m)	**C**	0.4774	0.2456	81	0.849	7.93	25.51
		F	0.4870	0.2427	8	0.950	3.02	7.42
6	Diskloading (kg/m^2)	**C**	1.681	0.3492	129	0.842	15.46	43.82
		F	0.5915	0.4958	17	0.971	7.45	20.28
7	Total Takeoff Power	**C**	0.1645	0.838	53	0.941	22.76	78.97
		F	1.062	1.144	10	0.981	15.66	22.76
8	Maximum continuous Power	**C**	1.14	0.764	36	0.90	21.62	74.65
		F	2.337	0.6715	8	0.76	14.40	35.55

Table 4.4: MTOW as a predictor variable in design trends for rotorcraft.

``

i. MTOW Vs Fuselage Length

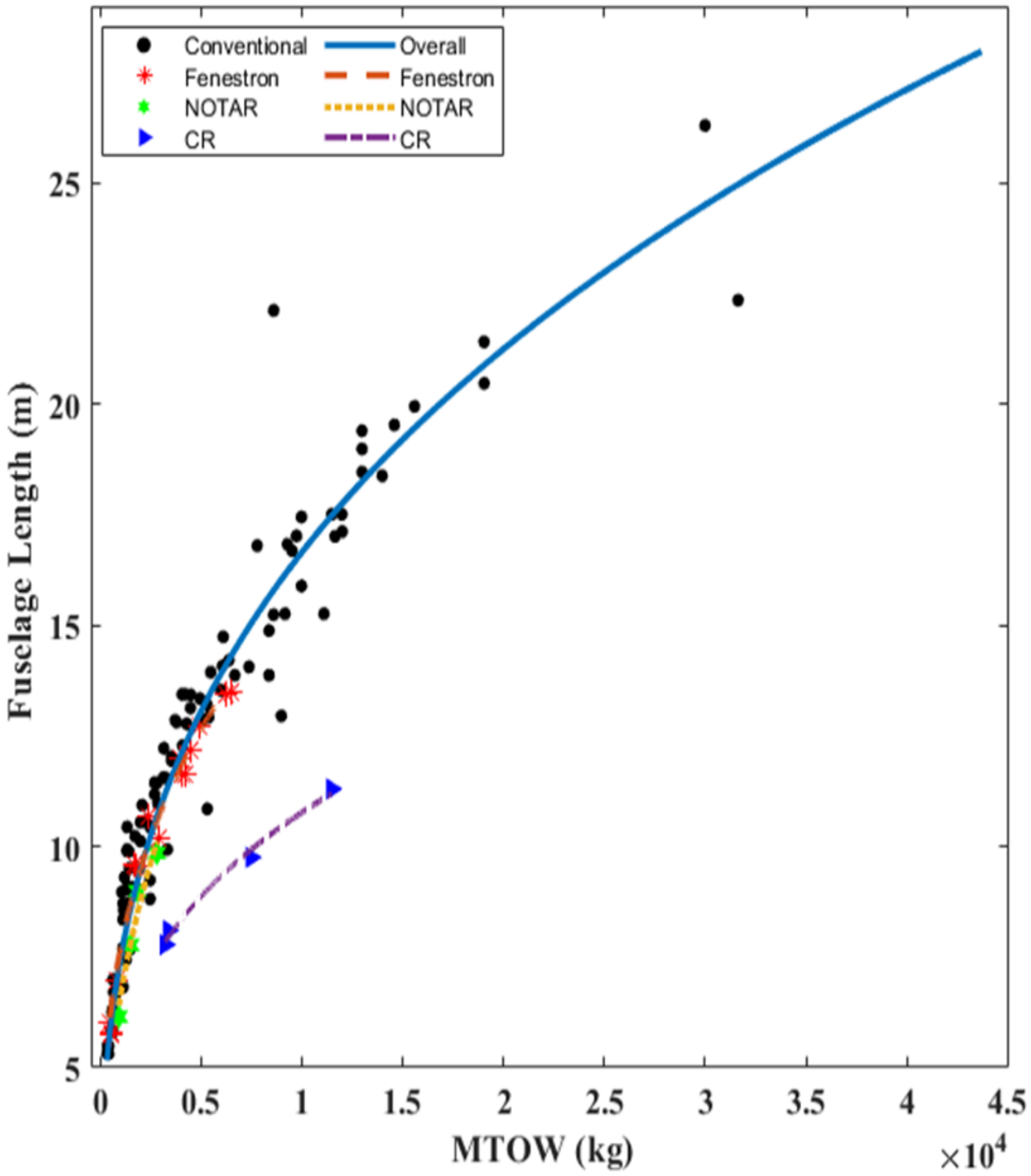

Figure 4-11: MTOW relation with fuselage length.

The trendline is sublinear between MTOW and fuselage length. It is increasing rapidly for comparatively lighter rotorcraft, but the gradient falls as MTOW increase above 4000 kg. Moreover, C-R has the smallest fuselage length in comparison to all other configuration

``

ii. MTOW Vs Empty Weight

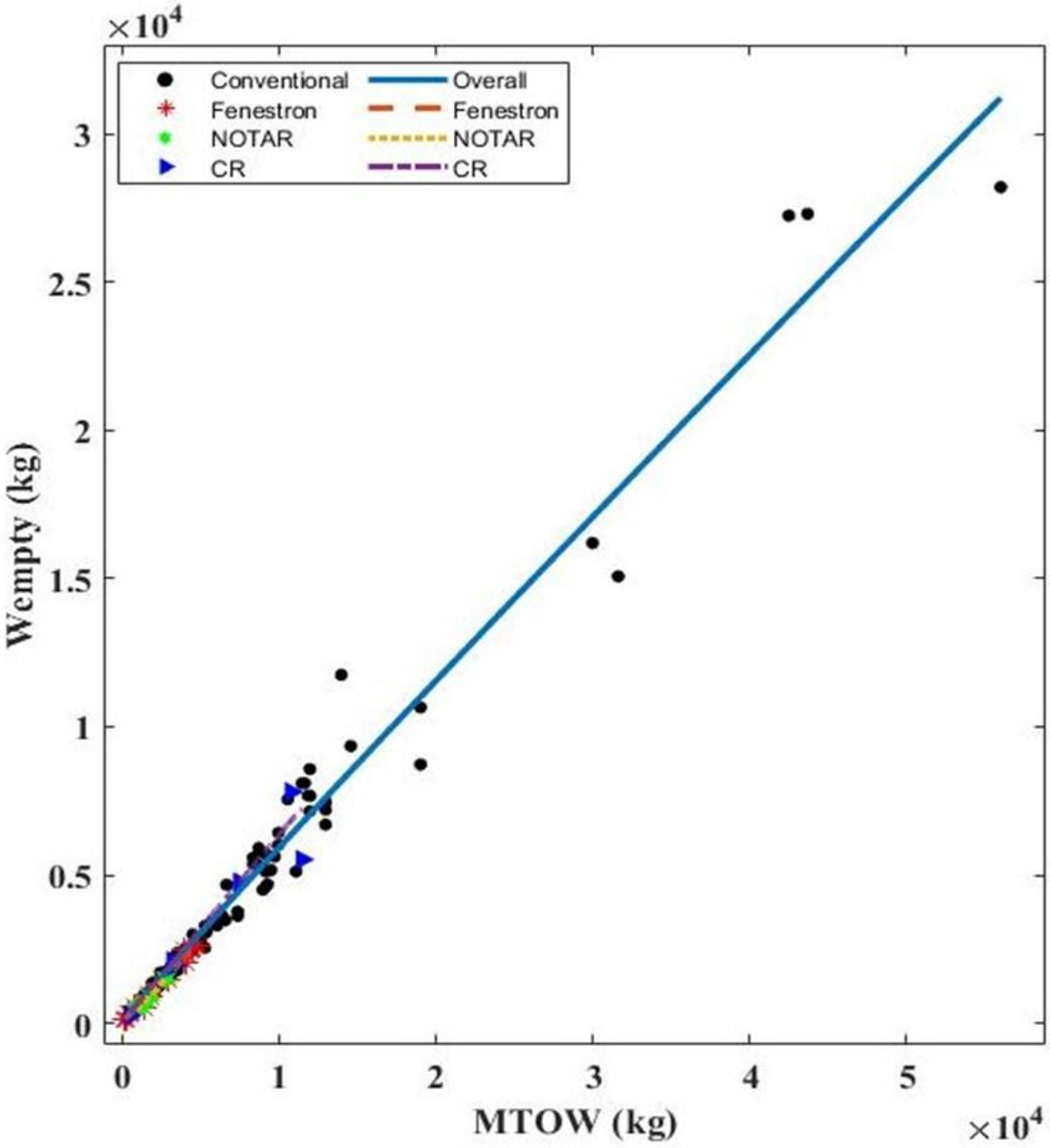

Figure 4-12: MTOW relation with an empty weight.

MTOW and Empty Weight are strongly correlated with an R-sq value of 0.97 for 155 entries.

The trendline is almost linear for all configurations except the NOTAR, which shows the superliner trend.

For any MTOW, rotorcraft below the trendline has a lower empty weight, which translates into a higher payload or fuel capacity; higher fuel capacity results in a more extended range.

On average, Empty weight is about 40-50 % of the maximum takeoff weight for Rotorcraft.

``

iii. MTOW Vs Main Rotor Diameter

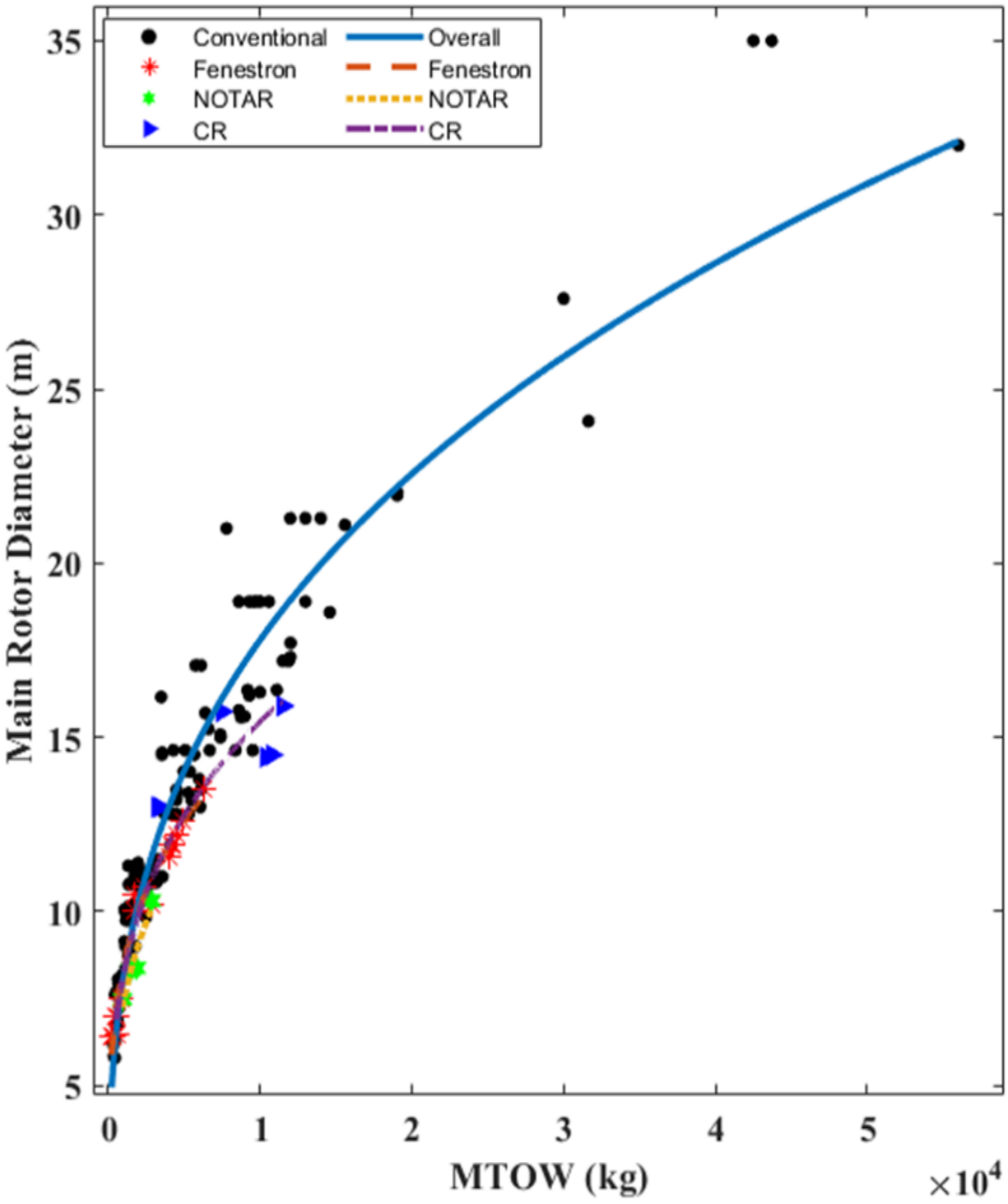

Figure 4-13: MTOW relation with main-rotor diameter.

Maximum takeoff weight and main rotor diameter are linked through the lift mechanism of the rotorcraft. The trendline is sublinear for all configurations, the gradient of the trend increases for lighter craft, but the gradient gradually drops as MTOW exceeds a certain limit

``

iv. MTOW Vs Height to the Main Rotor Head.

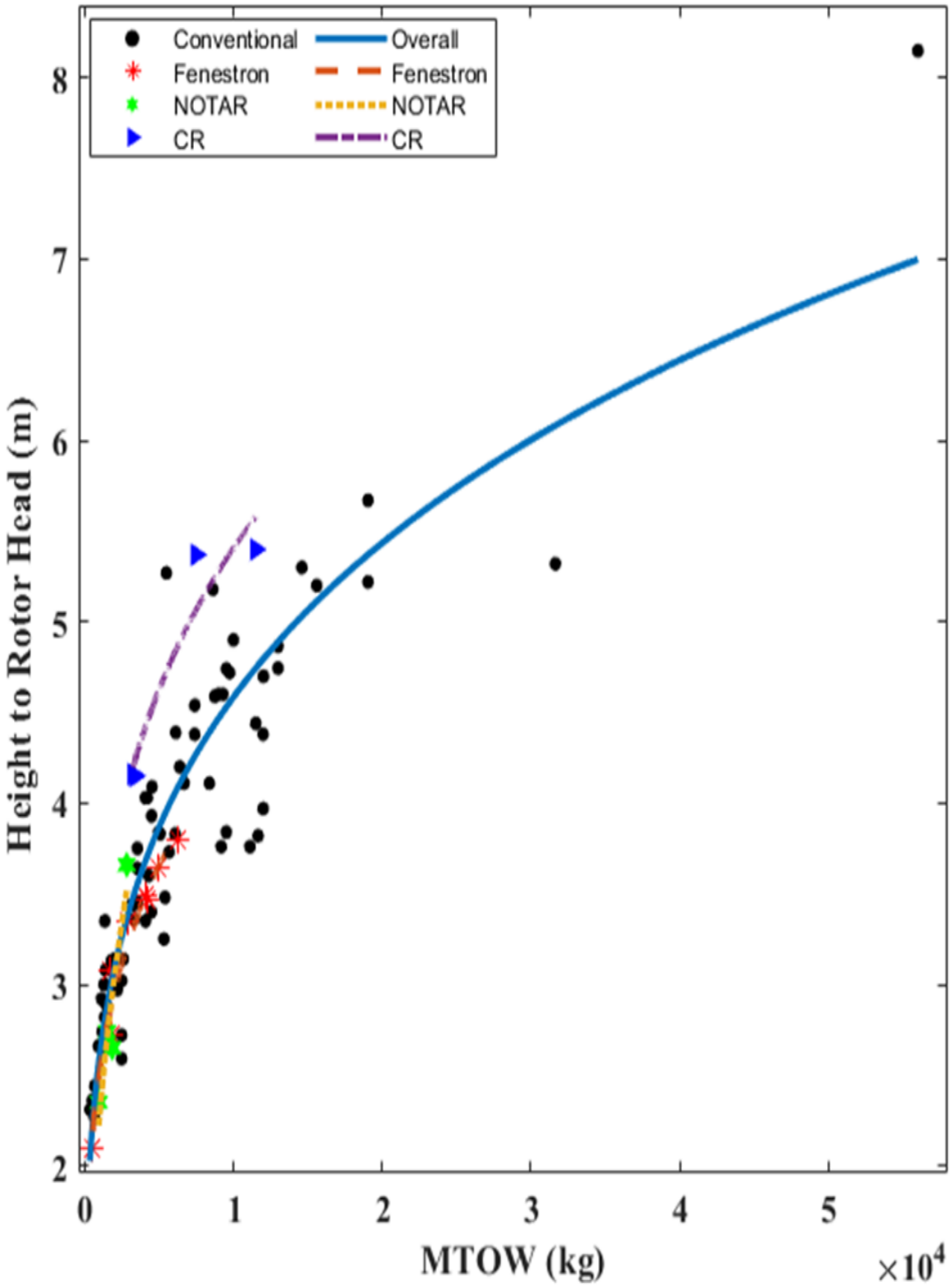

Figure 4-14: MTOW relation with height to the rotor head.

``

v. MTOW Vs Tail Rotor Diameter

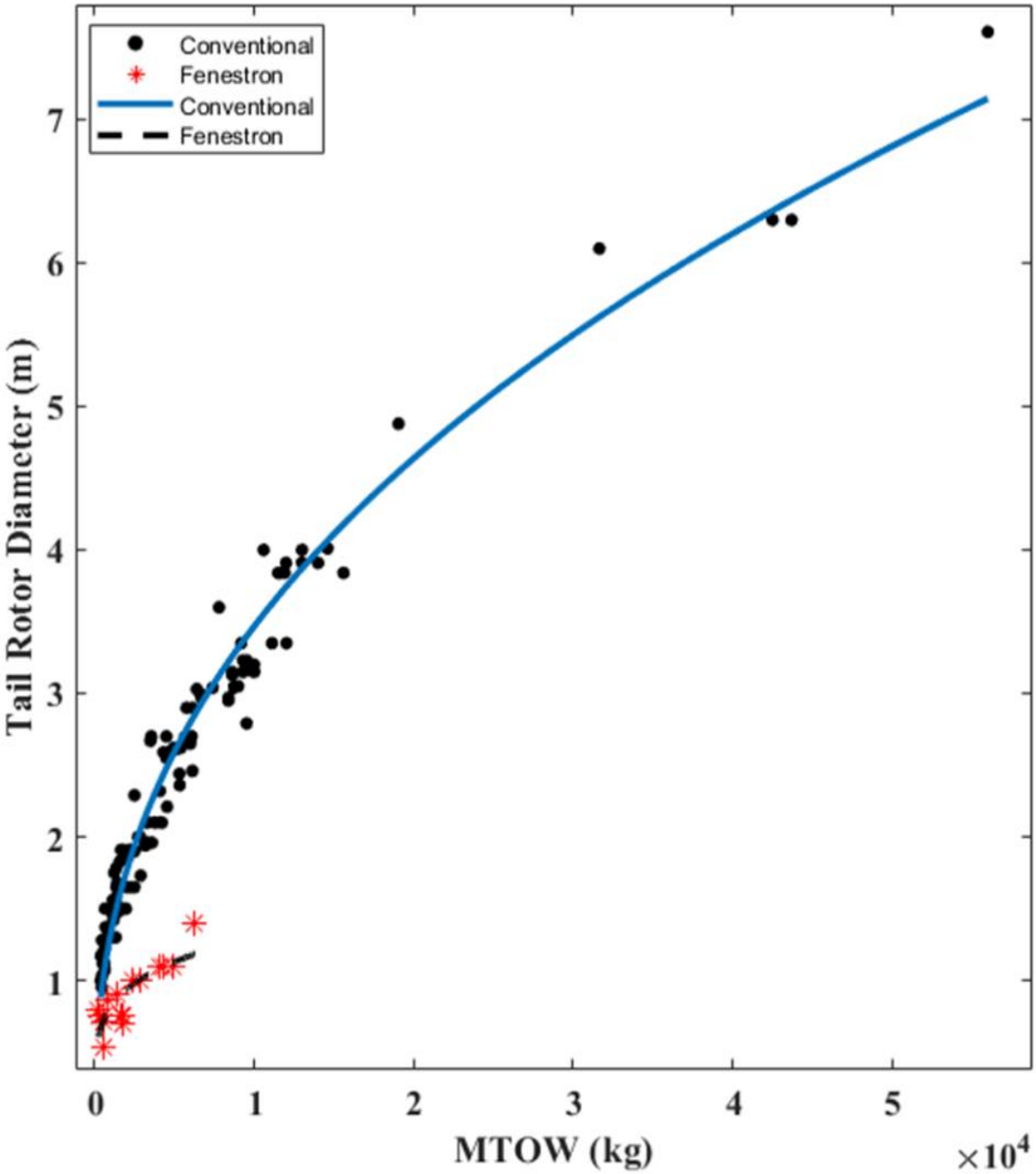

Figure 4-15: MTOW relation with tail rotor diameter.

The fenestron configuration's tail-rotor diameter is significantly less than conventional helicopters, even at the same MTOW.

For the same MTOW, the tail rotor diameter of conventional rotorcraft is about **50%-55%** larger in size compared to the fenestron counterpart. This signifies their compact size.

``

Config.	Name	Type	MTOW (kg)	Tail-Rotor diameter (m)	% Increase
F	HAI Z9-A	Light Utility	4100	1.1	52.58
C	Augusta A 129 Mangusta	Scout Helicopter		2.32	
F	Guimbal G2 Cabri	Two-seater helicopter	550	0.54	55
C	DFH Dragon 334	Two-seater helicopter		1.2	
F	Aerospatiale SA 341 Gazelle	Light Utility	1800	0.695	53.6
C	PZL SW-4	Light Utility		1.5	

Table 4.5: Tail rotor comparison of Fenestron and Conventional rotorcraft for same MTOW.

vi. MTOW Vs Diskloading

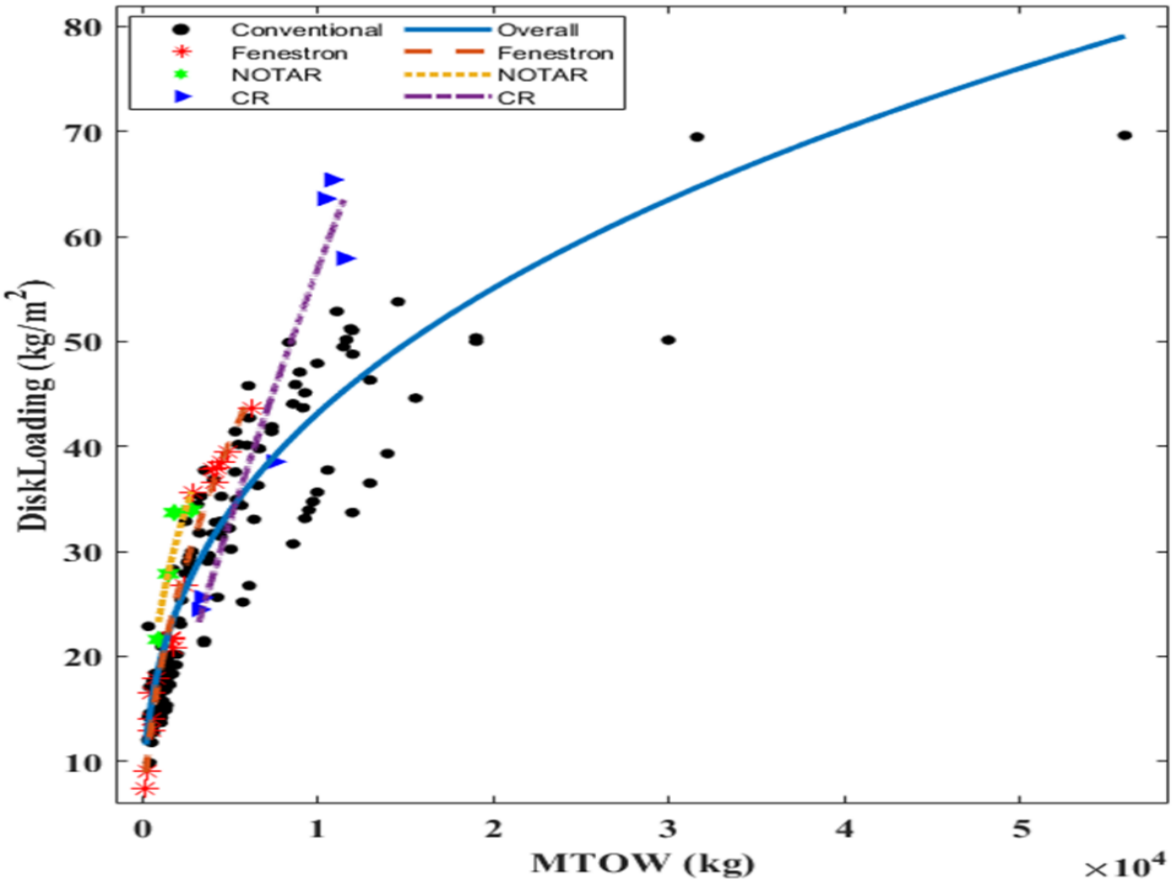

Figure 4-16: MTOW relation with diskloading.

``

vii. MTOW Vs Takeoff Power

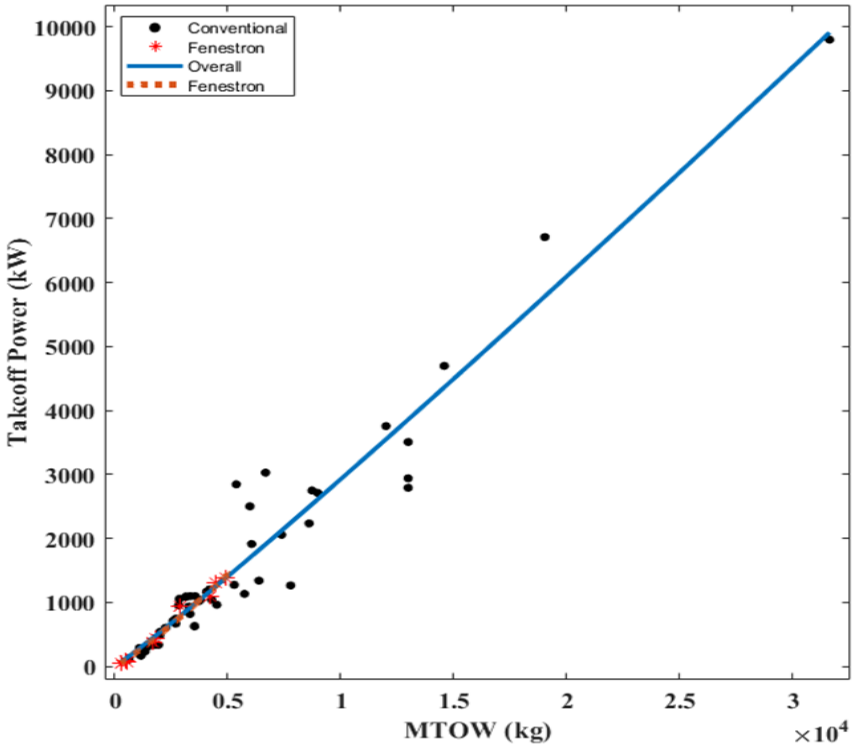

Figure 4-17: MTOW relation with takeoff power.

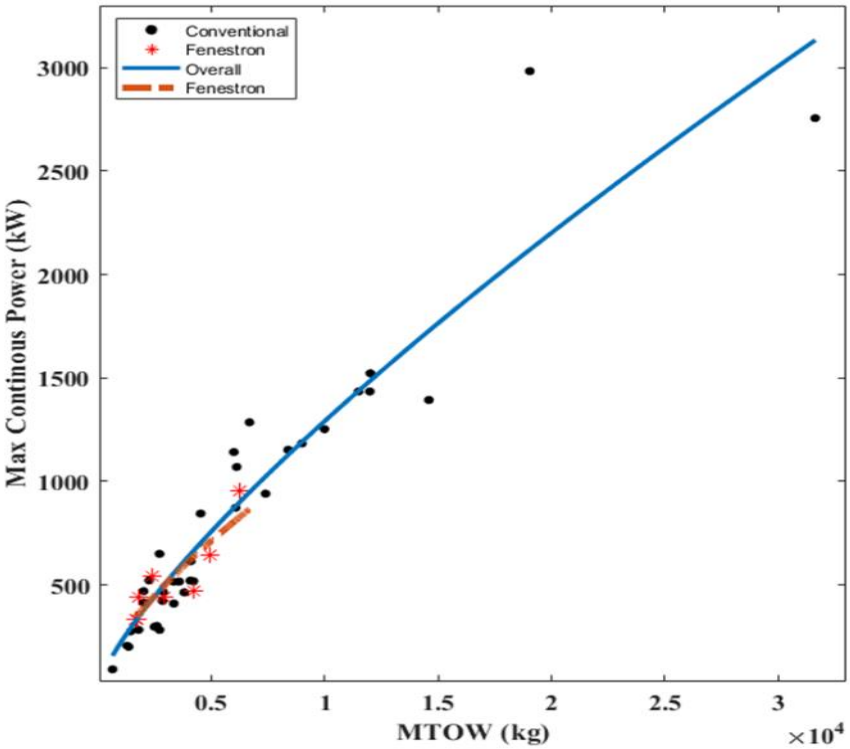

Figure 4-18: MTOW relation with maximum continuous power

``

MTOW versus Power relations shows a linear trend which is augmented by the fact that the heavier the aircraft gets higher would be thrust required to propel it.

III. Tail Rotor diameter as a primary independent variable

The primary function of the tail rotor is to counteract the torque produced by the main rotor and provide necessary yaw control. The thrust from the tail rotor, combined with the distance from the main rotor's center (primarily the tail boom), provides the necessary antitorque. The longer the tail rotor, the more effective it would be to counteract the torques; however, more extended tail booms add weight penalty; therefore, fuselage sizing is done following the tail rotor to give optimum antitorque and yaw control for a given power and maximum takeoff weight.

Tail rotor diameter and height to the rotor hub relation is a non-performance design constraint. Larger tail rotors are more effective, but they necessitate more considerable hub heights to prevent the tail rotor from scratching on the ground.

Design trends with tail rotor diameter as a predictor variable are summarized in table 4.6.

Power Law: $Y = \alpha \times X^{\beta}$								
Predictor X: Tail-Rotor Diameter								
S.No	**Response (Y)**	**Config**	**α**	**β**	**N**	**R-Sq**	**MAPE**	**Max. E**
1	Fuselage Length (m)	**C**	6.068	0.8212	98	0.70	14.0	34.40
		F	10.42	0.8948	13	0.909	8.58	33.36
2	Height to Rotor Head (m)	**C**	2.225	0.5714	79	0.843	7.59	31.33
		F	3.311	0.5433	8	0.913	3.94	12.81

Table 4.6: Tail-rotor diameter as predictor variable in design trends for rotorcraft.

``

i. Tail Rotor Diameter Vs Height to the Main Rotor Head

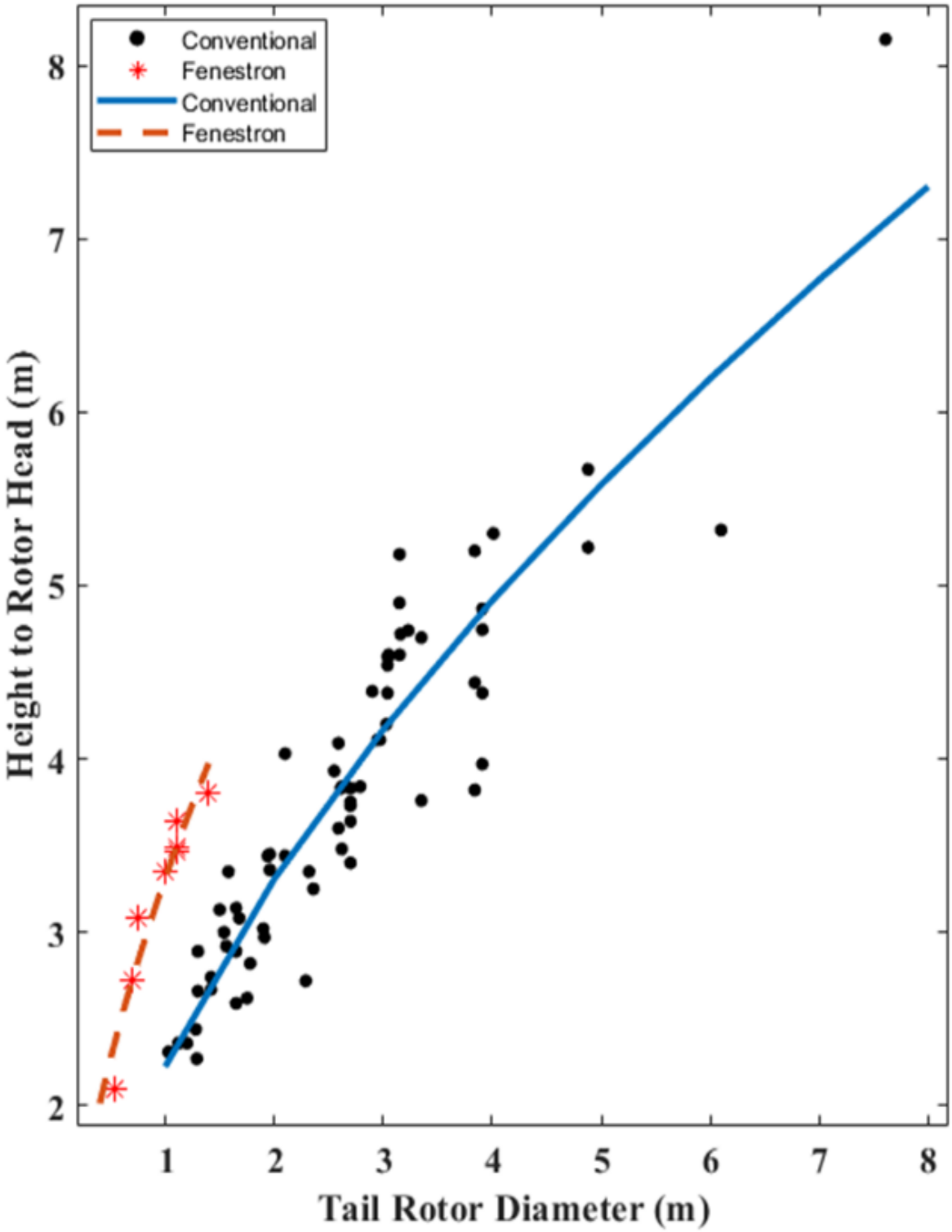

Figure 4-19: Tail-rotor diameter relation with height to the rotor head.

``

ii. Tail Rotor Diameter Vs Fuselage Length

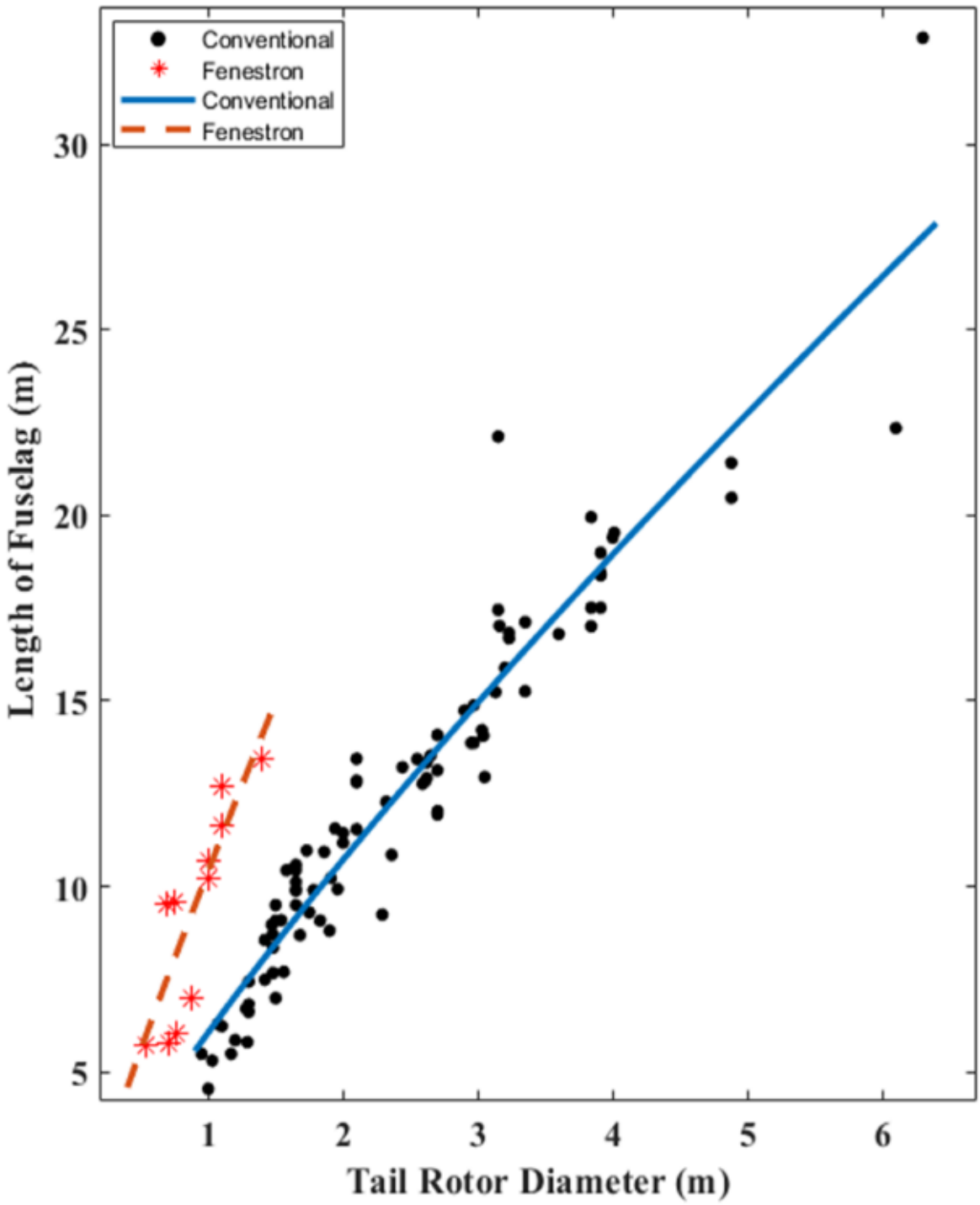

Figure 4-20: Tail-rotor diameter relation with fuselage length.

``

4.3 Performance Estimation through Surrogate Models

During the conceptual design phase, single variable models/design trends in conjunction with pre-existing semi-empirical relations estimate aircraft weight and geometric parameters. Additionally, these design trends assist in determining interdependencies among aircraft/rotorcraft design parameters and provide initial design bounds for preliminary sizing. However, estimating aircraft performance parameters using one explanatory variable is not entirely definitive when initial estimation is a goal. Suppose a parameter is calculated using more than one independent variable. In that case, the result will be much more conclusive and will help in significantly cutting down design iterations during the initial stages.

I. Range

It is the maximum distance that an aircraft or rotorcraft can fly between takeoff and landing for given takeoff weight and given amount of fuel.

For rotorcraft:

$$R = \int_{W_{GTOW}}^{W_{G_{TO}W-W_F}} \frac{V}{P \times SFC} dw$$

Where V is cruise velocity, P is power required that varies with density and gross takeoff weight, SFC is specific fuel consumption of engine(s) which is an important figure of merit that suggest how efficiently the engine convert fuel into power, W_{GTOW} and W_F are gross takeoff weight and initial fuel weight, respectively.

For propellor driven aircraft:

$$R = \frac{\eta pr}{g \times SFC} \frac{L}{D} ln \frac{W_0}{W_1}$$

ηpr_∞ is propellor efficiency, L/D is lift to drag ratio also called aerodynamic efficiency, Wo is gross takeoff weight whereas W1 is gross takeoff weight minus the fuel weight.

For Jet aircraft:

$$R = \frac{V}{ct} \frac{L}{D} ln \frac{W_0}{W_1}$$

V is cruise velocity whereas ct is thrust specific fuel consumption which indicates the fuel efficiency of an engine with respect to thrust output.

``

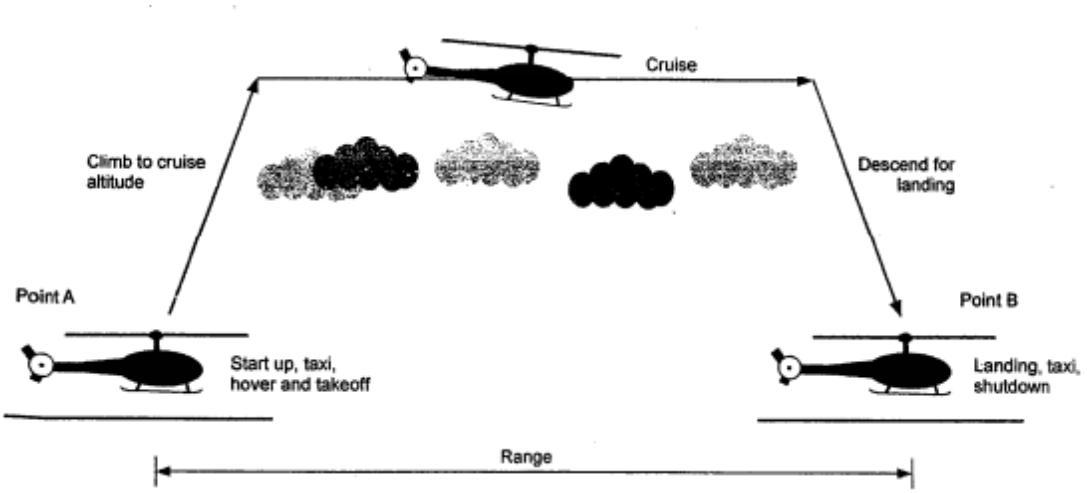

Figure 4-21: Range

	Surrogate Model	Statistical Results	
Rotorcrafts	Range = (0.1090×MTOW) + (0.764×V_{cruise}) + 0.635	**R^2 adjusted**	69.91
		R^2 predicted	68
		F	114.86
		N	99
	Range = (0.348×MTOW) – (0.161×Total Power) + (0.792×V_{cruise}) – 0.208	**R^2 adjusted**	73.32
		R^2 predicted	71.54
		F	86.21
		N	94
Propellor driven Aircraft	Range = (0.0696×MTOW) + (1.2203×Vcruise) + 0.0540	**R^2 adjusted**	78.78
		R^2 predicted	78.45
		F	572.64
		N	309
Jet driven Aircrafts	Range = (0.3342×MTOW) + (0.794×Vcruise) + 0.115	**R^2 adjusted**	74.86
		R^2 predicted	72.42
		F	66.61
		N	45
For all the relations mentioned above, $p<0.05$, VIF <10. Both independent and dependent variables are on a logarithmic scale			

Table 4.7: Surrogate model for Range.

``

II. Rate of Climb at Sea Level.

The rate of climb is defined as a change of altitude of an aircraft/rotorcraft concerning time. It is considered one of the most fundamental performance parameters in aeronautics, especially for combat aircraft. The rate of climb, often abbreviated as "ROC," is a function of air density and thus decreases with altitude. It can be analytically calculated using

Propellor driven:

$$(RoC)max = \frac{\eta_{pr}\,P}{W} - \left[\frac{2}{\rho_\infty}\sqrt{\frac{K}{3C_{D0}}}\left(\frac{W}{S}\right)\right]^{1/2} \times \frac{1.155}{(L/D)_{max}}\frac{2}{\rho_\infty}\frac{K}{3C_{D0}}\left(\frac{W}{S}\right)$$

Jet driven:

$$(RoC)max = \left[\frac{(W/S)Z}{3\rho_\infty C_{D0}}\right]^{1/2}\left[\frac{T}{W}\right]^{3/2}\left[1 - \frac{Z}{6} - \frac{3}{2(T/W)^2(L/D)^2_{max}\,Z}\right]$$

where

$$Z = 1 + \sqrt{1 + \frac{3}{(L/D)^2_{max}\,(T/W)^2}}$$

ROC of an aircraft is directly proportional to the excess power,where excess power is power available minus power required.In more general terms excess power is any reserve power that our engine has above whats's required to maintain level flight.

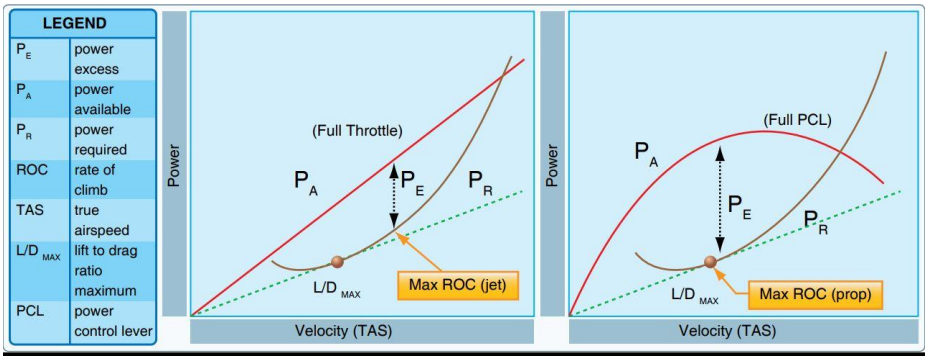

4-22: Graphical representation of ROC for a propellor and jet driven aircraft.

``

	Surrogate Model	Statistical Results	
Rotorcrafts	ROC = (0.112×Takeoff-Power) + (0.277×DiskLoading) + 2.48	$\mathbf{R^2}$ **adjusted**	59.56
		$\mathbf{R^2}$ **predicted**	56.97
		F	57.70
		N	78
	ROC = (0.396×Vmax) + (0.367×DiskLoading) + 1.747	$\mathbf{R^2}$ **adjusted**	69.43
		$\mathbf{R^2}$ **predicted**	65.94
		F	50.96
		N	45
Propellor driven Aircraft	ROC = (1.2052×Pa) – (1.2092×MTOW) + 3.6149	$\mathbf{R^2}$ **adjusted**	60.77
		$\mathbf{R^2}$ **predicted**	60.23
		F	315.51
		N	407
Jet driven Aircrafts	ROC = (2.598×logT/W) – (0.896×logb) + 5.205	$\mathbf{R^2}$ **adjusted**	82.51
		$\mathbf{R^2}$ **predicted**	79.10
		F	83.56
		N	36
For all the above-mentioned relations p<0.05, VIF <10. Both independent and dependent variables are on logarithmic scale			

Table 4.8: Surrogate model for Rate of climb at sea level.

III. Maximum Velocity at Sea Level.

It is defined as maximum horizontal velocity attained by an aircraft/rotorcraft for a given gross weight at a given altitude. The maximum velocity in level flight for jet-driven aircraft is calculated using:

$$V_{\max} = \left[\frac{\left[(T_A)_{\max}/W\right](W/S) + (W/S)\sqrt{\left[(T_A)_{\max}/W\right]^2 - 4C_{D0}K}}{\rho_\infty C_{D0}} \right]^{1/2}$$

TA/W is maximum thrust to weight ratio, also known as maximum thrust loading, W/S is wing loading, Cdo is zero-lift drag coefficient that accounts for both the skin friction drag and pressure drag, K is constant for the coefficient of drag due to lift

For Propellor driven aircraft's maximum velocity in level flight is calculated graphically.

``

For propellor driven:

$$P_A = T_A V_\infty$$

	Surrogate Model	Statistical Results	
Rotorcraft	Vmax = (0.331×MTOW) – (0.598×Main-Rotor Diameter) + 1.84	$\mathbf{R^2}_{\textbf{adjusted}}$	75.54
		$\mathbf{R^2}_{\textbf{predicted}}$	73.52
		F	98.29
		N	64
	Vmax = (0.328×DiskLoading) – (0.115×PowerLoading) + 1.957	$\mathbf{R^2}_{\textbf{adjusted}}$	77.12
		$\mathbf{R^2}_{\textbf{predicted}}$	74.72
		F	107.18
		N	64
	Vmax = (0.1848×DiskLoading) + (0.0731×Takeoff-Power) + 1.879	$\mathbf{R^2}_{\textbf{adjusted}}$	77.38
		$\mathbf{R^2}_{\textbf{predicted}}$	75.23
		F	108.76
		N	64
Propellor driven Aircraft	Vmax = (0.2326×b) – (0.6192×S) + (0.4166×Pa) + 2.0037	$\mathbf{R^2}_{\textbf{adjusted}}$	84.79
		$\mathbf{R^2}_{\textbf{predicted}}$	83.69
		F	335.23
		N	195
Jet driven Aircrafts	Vmax= T– (0.4030×b) + 3.0015	$\mathbf{R^2}_{\textbf{adjusted}}$	90.40
		$\mathbf{R^2}_{\textbf{predicted}}$	87.90
		F	109.29
		N	36
For all the relations mentioned above, $p<0.05$, VIF <10. Both independent and dependent variables are on a logarithmic scale			

Table 4.9: Surrogate model for the maximum velocity at sea level.

IV. Service Ceiling

Service ceiling represents the upper limit of steady-level flight. It refers to the density altitude at which the rate of climb of an aircraft drops to 100 ft/min. The Service ceiling of an aircraft/rotorcraft is calculated graphically by extrapolating the rate of climb and density relation

``

as shown in fig 4.22.

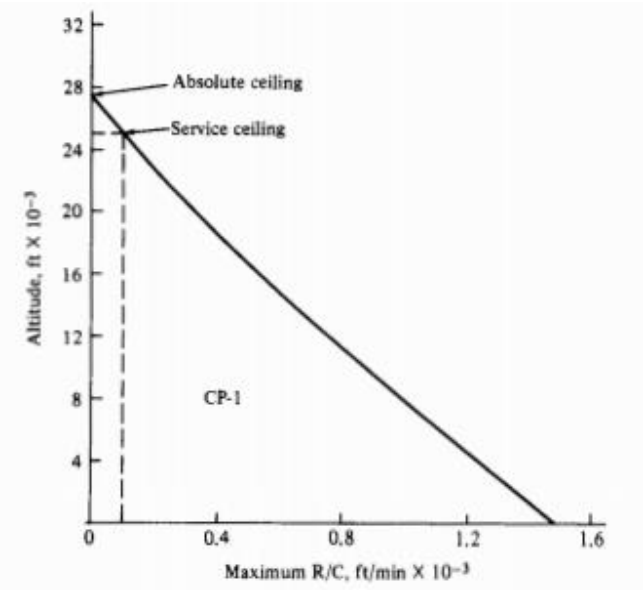

Figure 4-23: Service and Absolute Ceiling

The density altitude corresponding to the rate of climb of 100 ft/ min and 0 ft/min indicates the service ceiling and absolute ceiling of an aircraft, respectively.

	Surrogate Model	**Statistical Results**	
Rotorcraft	Service Ceiling= (0.0346×DiskLoading) + (0.5326× V_{cruise}) + 2.363	$\mathbf{R^2}_{\textbf{adjusted}}$	63.09
		$\mathbf{R^2}_{\textbf{predicted}}$	61.42
		F	75.35
		N	88
Propellor driven Aircraft	Service Ceiling = (0.704×b) – (0.6653×S) + (0.2916×Pa) + 3.1237	$\mathbf{R^2}_{\textbf{adjusted}}$	60.86
		$\mathbf{R^2}_{\textbf{predicted}}$	59.38
		F	105.70
		N	203
Jet driven Aircrafts	Service Ceiling = (0.3157×T) – (1.3134×h) + 4.4937	$\mathbf{R^2}_{\textbf{adjusted}}$	87.79
		$\mathbf{R^2}_{\textbf{predicted}}$	86.09
		F	141.24
		N	40
For all the above-mentioned relations $p<0.05$, VIF <10. Both independent and dependent variables are on logarithmic scale			

``

Table 4.10: Surrogate model for service ceiling.

V. Endurance

It is the maximum length of time that an aircraft stays in the air with a full load of fuel. Endurance is primarily affected by the fuel efficiency of an engine design, such as specific fuel consumption and thrust specific fuel consumption. Unlike Range, which focuses on distance traveled, endurance is mainly interested in the time an aircraft stays in the air.

Endurance for jet-driven aircraft is calculated using.

$$E = \frac{1}{C_t}\frac{C_L}{C_D} ln \frac{W_0}{W_1}$$

Here, ct is thrust-specific fuel consumption, L/D is lift to drag ratio also known as aerodynamic efficiency, for jet-propelled aircraft's maximum endurance is obtained by flying at maximum L/D.

Endurance for propellor driven aircrafts

$$E = \frac{\eta_{pr}}{c}\sqrt{2\rho_{\infty}S}\frac{C_L^{3/2}}{C_D}(W_1^{-1/2} - W_0^{-1/2})$$

η_{pr} is propellor efficiency, c refers to the specific fuel consumption, whereas $W_1^{-1/2} - W_0^{-1/2}$ represents fuel capacity of an aircraft, for propellor driven aircraft maximum endurance is achieved by flying at $\frac{C_L^{3/2}}{C_D}$, maximizing fuel capacity and minimizing specific fuel consumption

4.4 Dimensionality Reduction.

Maximum takeoff weight, Thrust/Power available, cruise velocity, wing-span, and wing-area are observed to be the key predictor variables to estimate aircraft performance parameters. Similarly, for rotorcraft, key predictor variables are Maximum takeoff weight, cruise velocity, main rotor diameter, takeoff/maximum continuous power, disk loading, and power loading, which are quite in line with the analytical equation function shown in table 8. However, quite interestingly, aircraft height emerged as a unique predictor to estimate service ceiling for which there is no adequate theoretical explanation.

``

We now reach an exciting conclusion that we can build models with fewer parameters and still predicts the performance parameters to a high level of accuracy. Moreover, time exhaustive calculations of aerodynamic parameters and lift to drag ratios in the initial phase of developing specification model can be avoided as prediction via weight, geometric, and propulsion parameters still suffice for the initial stages. Dimensionality reduction in surrogate models is summarized in table

Parameters	Analytical equation function	Surrogate model function
Maximum Velocity	$V\max = f(T/Pa, W, S, Cdo, k, \rho\infty)$	$Vmax = f(T/Pa, S, b)$
Range	$Range = f(V\infty, TSFC/SFC, \eta pr, L/D, Wo, W1)$	$Range = f(Wo, Vcruise)$
Ceiling	$Ceiling = f(W, S, T/Pa, \rho\infty, L/D, Cdo)$	$Ceiling = f(T/Pa, S, b, h)$
Rate of Climb	$ROC = f(W, S, T/Pa, \rho\infty, L/D, Cdo)$	$ROC = f(T/Pa, S, b)$

Table 4.11: Dimensionality Reduction in analytical equations through surrogate models

4.5 Accuracy of Surogate Models for the unseen data .

In order to assess the prediction accuracy of the surrogate model..Performance parameters estimated through surrogate models are compared with actual values reported in their OEM (original equipment manufacturer) as shown in fig 4.23. The results were quite optimistic for both fixed-wing and rotorcraft as, with just a few exceptions, the difference between surrogate estimation and actual value is less than almost 30 %.

``

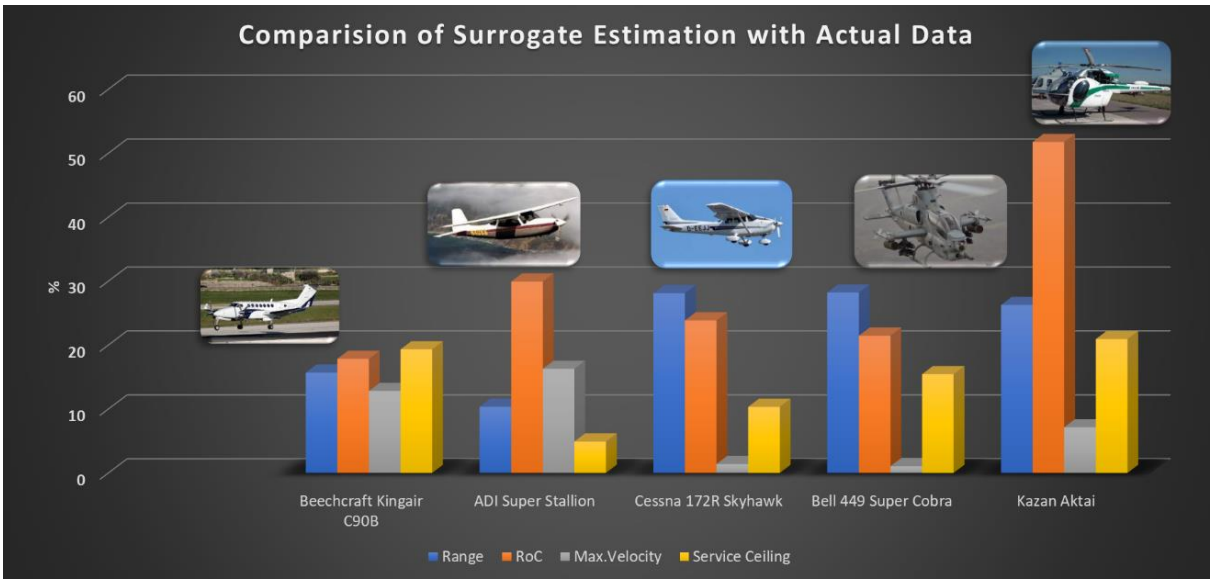

4-24: Comparision of surrogate estimation with actual data

CHAPTER 5: **Biomimicry**

Biomimetics or biomimicry is a new science in which we seek nature-inspired solutions to many complex human problems. The evolutionary process stretched over millions of years has yielded some elegant, robust, and efficient designs. These marvelous designs are the motivation behind biomimetics. Though biomimicry was first coined in 1997, humanity has always looked to nature to learn, innovate, design, and build. Some of the fascinating examples of biomimicry are summarized below.

5.1 Velcro

Swiss engineer George de Mistral invented Velcro in 1948. He went hiking with his dog; upon return, he noticed burrs clung to his cloth. He studied those hooks like biostructures under a microscope and realized their commercial application; thus, after more than eight years of extensive research, he came up with this ingenious design widely used everywhere, from the spacesuit to handbags.

``

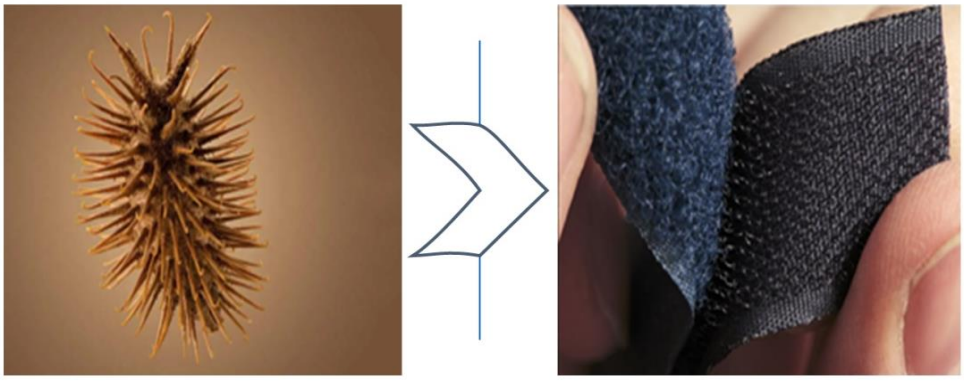

Figure 5-1: Burrs and Velcro.

5.2 Moth eye and Solar panels

Photovoltaics are used to convert sunlight into electricity. However, during this process, it reflects a lot of solar energy in the form of heat; this results in an efficiency drop. Scientists came up with an ingenious solution inspired by the moth's eye to overcome this practical problem. Moth eyes have textured patterns and are covered in nano tapered structures. These tiny posts absorb most of the light without reflection; this gives moth better night vision along with anti-glimmer, which otherwise would have to attract predators. Scientists have mimicked the biostructure of moth eyes to develop a coating for solar cells which could absorb the maximum amount of solar energy.

Figure 5-2: Moth eyes and Solar Panels.

5.3 Bullet train and kingfisher

Bullet trains are engineering marvels of the 20th century; traveling at a terrific speed of about 300 kph causes severe noise problems, especially while exiting the typical train tunnels. In

``

late 1990, Japanese engineers came up with an ingenious solution to overcome the noise problem. They noticed a kingfisher, a bird with a long beak that hovers above the water to watch its prey, then dives into the water slicing through it with little or no splash. Its bill's aerodynamic design and the ease and speed with which it catches its prey inspired the engineers to redesign the bullet train nose. Quite surprisingly, the new design inspired by king fisher results in quitter train, but its streamlined design has increased its speed by 10% and reduced electricity consumption by 15%.

Figure 5-3: King Fisher and Bullet Train

5.4 Stenocara bettle and water collection

Scientists have devised an innovative solution inspired by the Nambia beetle (stenocardia beetle) to deal with water shortages in dry areas. It is a long-legged, berry-sized insect, and it collects the water from the atmosphere by fog basking that is by leaning its bumpy abdomen into the foggy wind. The collected droplets are then channeled down into its mouth through its hardened shell containing tiny grooves and bumps; after a considerable amount of research, scientists have borrowed this nature-inspired water collection solution to make water collection nets and liquid collecting permeable structures.

``

Figure 5-4: Stenocara beetle and Fog collecting nets.

5.5 Biomimicry in Aviation.

Humans have long been intrigued with bird's ability to fly. For many hundred years, humans have mimicked birds to fly. The wing design in aircraft itself was first inspired by birds.

Figure 5-5: Biomimicry in aviation.

The aerospace industry has long embraced Biomimicry. The Airbus A300-600ST, popularly known as "beluga," is evident that nature has taught us some exceptional design innovations to invent aerospace marvels like the beluga super transporter. Similarly, In 2013, Airbus integrated new Sharklet technology into its A320 Family. Sharklets are vertical wingtip extensions that resemble dorsal fins on sharks. These sharklets reduce induce drag which in turn reduce fuel consumption by about 4%.

Some of the interesting futuristic bioinspired aerospace projects are summarized below:

``

Fello'fly: formation flight observed by migrating birds has always inspired aerospace engineers to mimic and harness associated benefits for aviation industry. In formation flights the trailing bird flies in the upwash region of the leading bird this way it harness the wake energy of the upwash for lift which is why it is often called wake energy retrieval. Airbus fello'fly project aims to realize the formation flying in transport aircrafts. It is expected that by employing a fello'fly in transport aircrafts we can reduce fuel consumption by 5-10% per trip which in turn will reduce CO2 emission by 3-4 million tons per year.

Figure 5-6: Formation flying.

Bird of Prey: To encourage next-generation aerospace engineers to explore a bioinspired innovative solution to develop sustainable, cleaner, greener, and more quitter aircraft. Airbus has revealed its bird-like conceptual airline design known as "Bird of prey." The blended wing to fuselage joint mimics the graceful arch of falcon or eagle, combining both strengths with aerodynamic efficiency. The wing tip is designed to look like an eagle's intricate feathers, resulting in a multifunctional, active structure that provides roll stability while reducing drag. Unlike the vertical tail of conventional aircraft, birds of prey would have split tails for fine control resulting in considerable drag reduction.

``

Figure 5-7: Bird of prey.

5.6 Comparative study of geometric trends in birds and fixed-wing aircraft

For millions of years, nature has perfectly engineered birds for different mission profiles. e.g., high aspect ratio wings in albatross, gulls, and gannets are suitable for gliding over long distances. Eagles, hawks, and storks are equipped with broad and slotted feathers for soaring and climbing upward currents of air, crows Robins, blackbirds, and sparrows have short, elliptical wings which offer the advantage of flying in dense forest where a quick burst of speed is required to catch the prey and escape the predator. Similarly, falcons are equipped with long, slender wings suitable for high-speed, long-distance travel.

It is pretty insightful to investigate and compare design trends in aircraft and birds since natural flyers have always offered efficient design prospects to implement in aircraft design. In fact, wing design itself is first from birds.

Comparative study of design trends in nature and technology are shown below

``

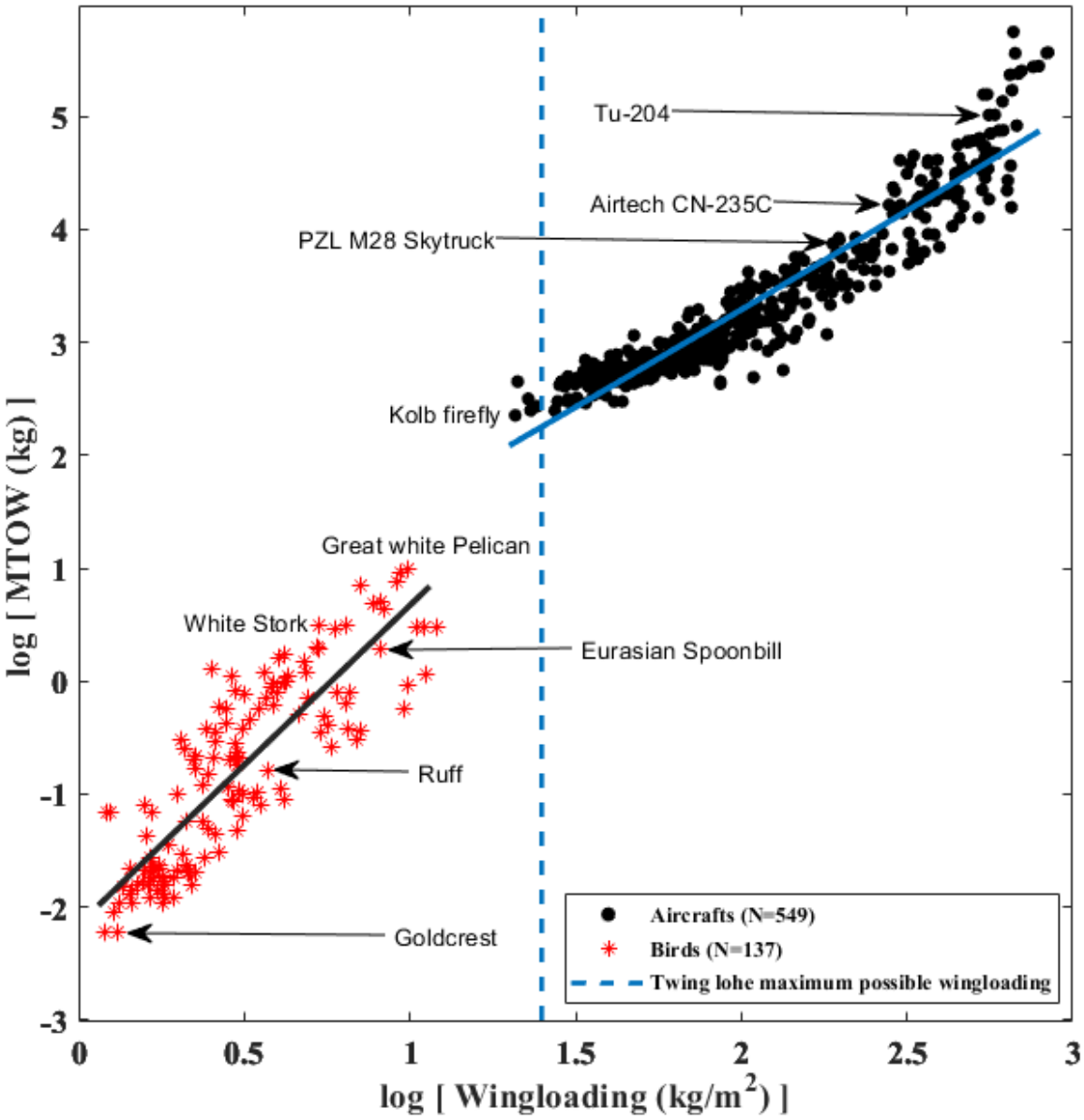

Figure 5-8: A comparative study between birds and aircraft. MTOW Vs. Wingloading"

The relationship between MTOW and wing-loading is plotted for a dataset of 686 entries, including 549 aircraft and 137 birds belonging to nearly every category, ranging from soaring, gliding, and flapping birds to all aircraft categories listed in table 1. On a log-log scale, wing-loading and maximum take-off weight grow almost linearly for natural and artificial flyers. Moreover, the gliding birds and the motor-gliders lie above the trend line, whereas fighter and fast-flying birds lie below the line. The vertical line at 25 kg/m^2 represents the maximum wing-loading constraint for birds, the point beyond which birds become too heavy to fly.

``

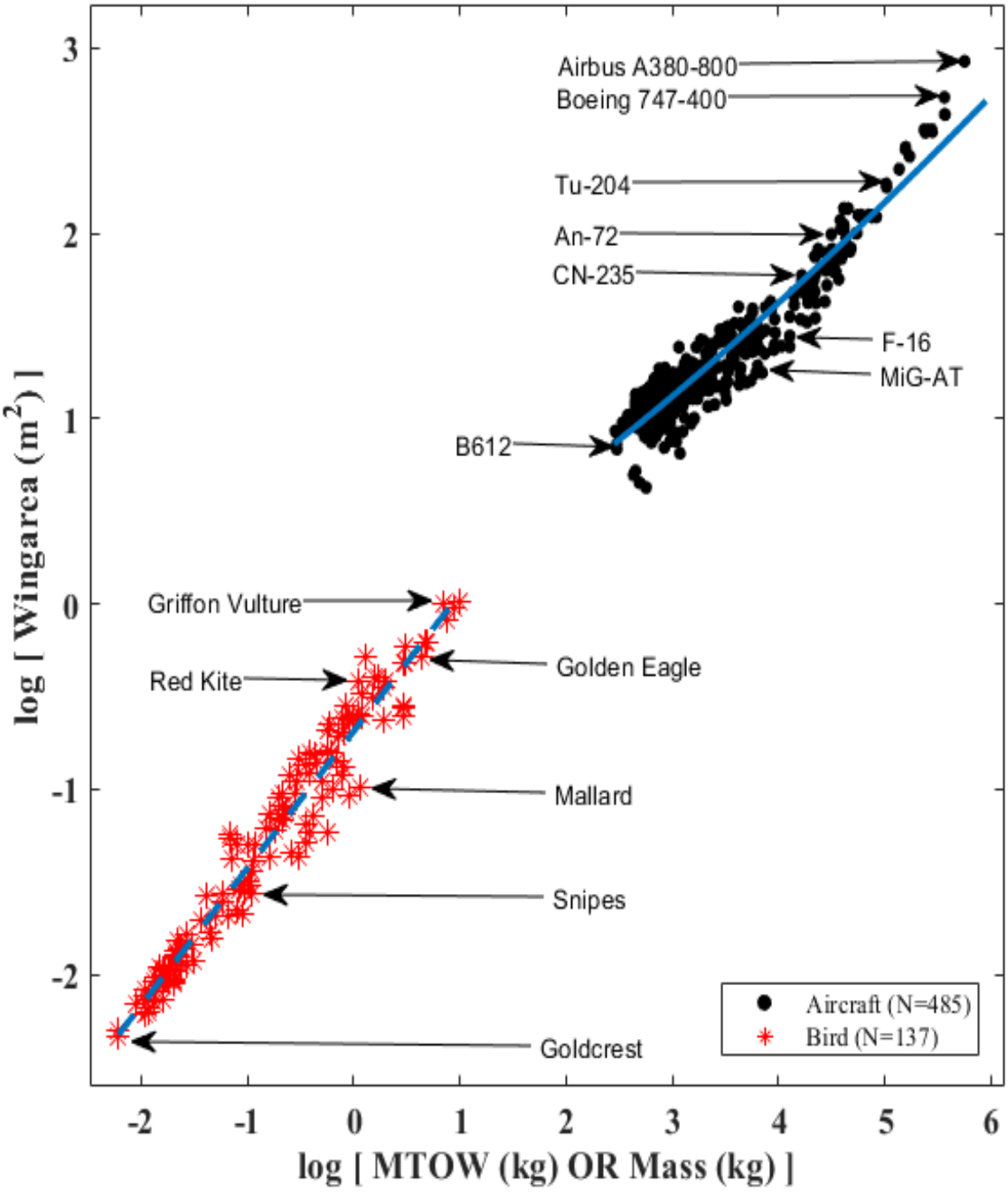

Figure 5-9: A comparative study between birds and aircraft. "MTOW Vs. Wing area"

Figure 5.10 depicts the relationship between MTOW and wing-area for 643 data points, including 137 birds and 485 aircraft. The trendline for birds grows faster than aircraft, implying that lift generation birds rely more on their wing area than velocity (dynamic lift).

``

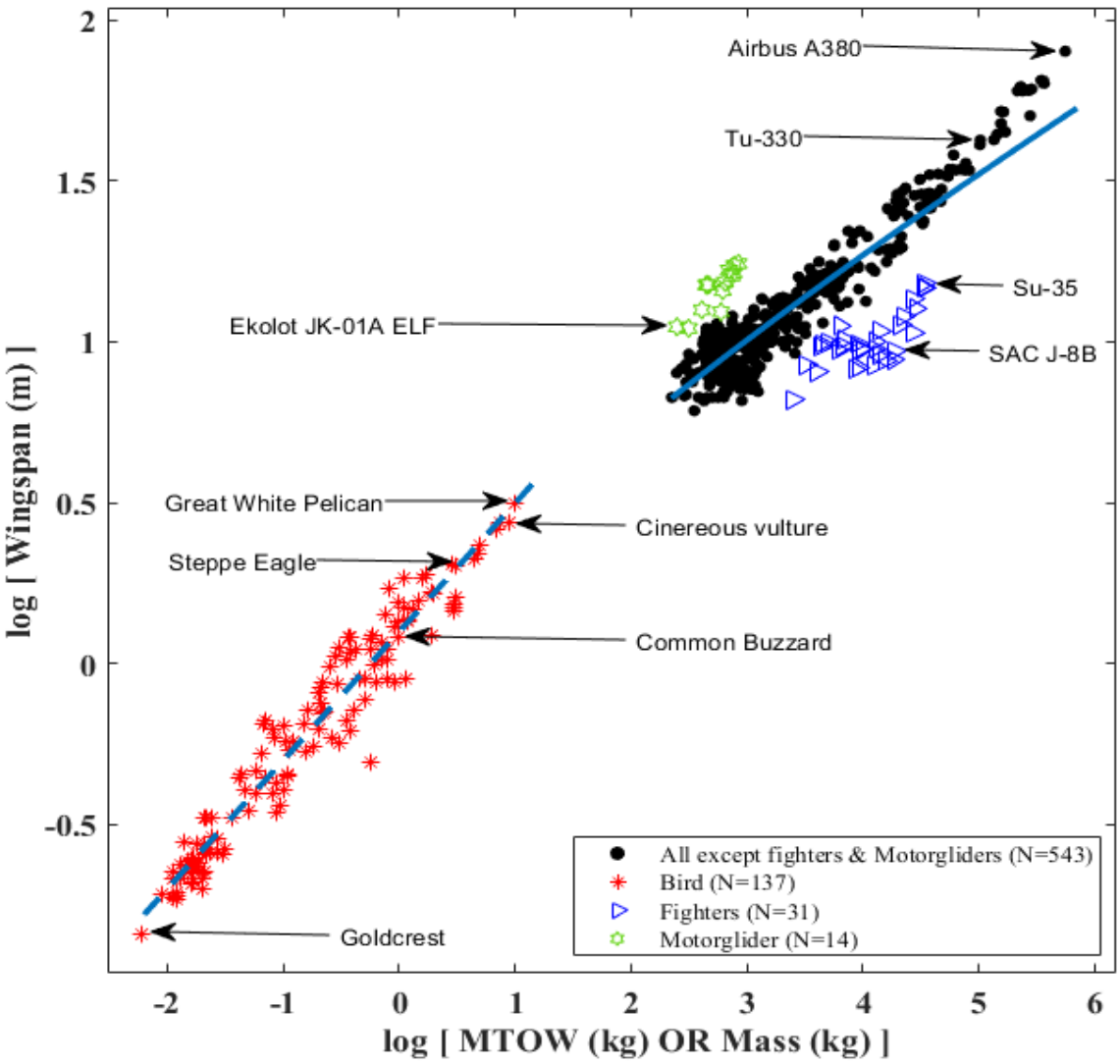

Figure 5-10: A comparative study between birds and aircraft.“MTOW Vs. Wingspan”

Figure 5.11 shows the relationship between MTOW and wingspan. The scope of the graph extends from one of the smallest passerine birds, “Goldcrest,” weighing about 0.006 kg at one end, to one of the largest passenger aircraft, “Airbus A380,” weighing about 560000 kg at the other ends. Interestingly, both birds and fixed-wing aircraft follow scalability law in their design; nevertheless, birds adhere to the trendline more strictly than aircraft. Furthermore, the relation is linear and highly correlated; however, motor-gliders and fighters diverge from the trendline.

``

CHAPTER 6: **CONCLUSION**

This research discusses three critical aspects of aircraft and rotorcraft design. The first part explores design trends for estimating aircraft/rotorcraft geometric, weight, and propulsion parameters during preliminary sizing; additionally, the scaling law used to develop design trends will help us comprehend how aircraft/rotorcraft parameters grow in proportion to their weight. The second part is intended to learn, inspect, and implement various design prospects from nature, for which a comparative study of scaling laws in nature and technology is presented. The third part offers surrogate models to predict the aircraft and rotorcraft performance parameters to an adequate confidence level during the initial design cycle when a rapid design assessment is more important than analysis fidelity. However, it is to mention that these techniques are not meant to replace but to complement the pre-existing methods. The idea behind the surrogate-based estimation is to cut down the initial iterations to reach the specification model of the design process. Once the specification model building time is cut down, the designers will focus on the computational models and verification/validation process. Moreover, these stated techniques will also be helpful for the strategic organization in estimating the adversary's aircraft to a higher confidence level for further tailoring the counter-strategies.

``

References

1. Newman, M.E., *Power laws, Pareto distributions and Zipf's law.* Contemporary physics, 2005. 46(5): p. 323-351.
2. West, G.B., J.H. Brown, and B.J. Enquist, *The origin of universal scaling laws in biology.* Scaling in biology, 2000: p. 87-112.
3. Bettencourt, L.M., et al., *West. 2007. Growth, innovation, scaling, and the pace of life in cities.* Proceedings of the National Academy of Sciences. 104(17): p. 7301.
4. Moore, G.E., *Cramming more components onto integrated circuits*. 1965, McGraw-Hill New York, NY, USA:.
5. Tennekes, H., *The simple science of flight: from insects to jumbo jets*. 2009: MIT press.
6. Anderson, J.D., *Aircraft performance & design*. 1999: McGraw-Hill Science Engineering.
7. Lim, J.-H., S.-J. Shin, and J.-M. Kim, *Development of an advanced rotorcraft preliminary design framework.* International Journal of Aeronautical and Space Sciences, 2009. 10(2): p. 134-139.
8. Rand, O. and V. Khromov, *Helicopter sizing by statistics.* Journal of the American Helicopter Society, 2004. 49(3): p. 300-317.
9. Lier, M., *Statistical methods for helicopter preliminary design and sizing.* 2011.
10. Sullivan, T., M.A. Meyers, and E. Arzt, *Scaling of bird wings and feathers for efficient flight.* Science advances, 2019. **5**(1): p. eaat4269.
11. Roskam, J., *Airplane design*. 1985: DARcorporation.
12. Gudmundsson, S., *General aviation aircraft design: Applied Methods and Procedures*. 2013: Butterworth-Heinemann.
13. Raymer, D., *Aircraft design: a conceptual approach*. 2012: American Institute of Aeronautics and Astronautics, Inc.
14. Kundu, A.K., M.A. Price, and D. Riordan, *Conceptual Aircraft Design: An Industrial Approach*. 2019: John Wiley & Sons.
15. Johnson, W., *Rotorcraft aeromechanics*. Vol. 36. 2013: Cambridge University Press.
16. Queipo, N.V., et al., *Surrogate-based analysis and optimization.* Progress in aerospace sciences, 2005. 41(1): p. 1-28.
17. Han, Z.-H. and K.-S. Zhang, *Surrogate-based optimization.* Real-world applications of genetic algorithms, 2012. 343.
18. Gallaher, P.D., R.A. Hunt, and R.C. Williges, *A regression approach to generate aircraft predictor information.* Human Factors, 1977. 19(6): p. 549-555.
19. Ghasemi Hamed, M., et al. *Statistical prediction of aircraft trajectory: regression methods vs point-mass model*. 2013. ATM Seminar.
20. Othman, N. and M. Kanazaki. *Efficient Flight Simulation Using Kriging Surrogate Model Based Aerodynamic Database*. in *53rd AIAA Aerospace Sciences Meeting*. 2015.
21. Ashraf, M.A., *Modeling of Scalability Laws for Unmanned Air Vehicles*. 2016, National University of Sciences and Technology.
22. Javad, S.M.T., *Surrogate Modeling of Aircraft Performance*. 2017, National University of Sciences and Technology.
23. Jackson, P., *Jane's all the world's aircraft 2007–2008.* Jane's Information Group, 2007: p. 2007-2008.
24. Oliver, D., *Jane's Helicopter Markets and Systems*. Issue.

``

25. Bruderer, B. and A. Boldt, *Flight characteristics of birds: I. Radar measurements of speeds.* Ibis, 2001. 143(2): p. 178-204.
26. Chenglin, Z., *New Developments of Helicopter Technology [J]*. Transactions of Nanjing University of Aeronautics & Astronautics, 1997. 6.
27. Leishman, G.J., *Principles of helicopter aerodynamics with CD extra*. 2006: Cambridge university press.
28. Gay, D. and S.V. Hoa, *Composite materials: design and applications*. 2007: CRC press.
29. Newman, R., *The Technical, Aerodynamic & Performance Aspects of a Helicopter: A Manual for Helicopter Pilots and Engineers Who Want to Know More*. BookBaby. 566.
30. Corda, S., *Introduction to aerospace engineering with a flight test perspective*. 2017: John Wiley & Sons.
31. Sampatacos, E., K. Morger, and A. Logan. *NOTAR-The viable alternative to a tail rotor*. in *Aircraft Design, Systems and Technology Meeting*. 1983.
32. Torenbeek, E. and H. Wittenberg, *Flight physics: essentials of aeronautical disciplines and technology, with historical notes*. 2009: Springer Science & Business Media.
33. Dancey, C.P. and J. Reidy, *Statistics without maths for psychology*. 2007: Pearson education.
34. Schinazi, R.B., *Multiple Linear Regression. Handbook of Psychology*. John Wiley & Sons, Inc, 2012. 2012(364-368): p. 4.
35. *Multiple Regression Analysis: Use Adjusted R-Squared and Predicted R-Squared to Include the Correct Number of Variables*. Available from: https://blog.minitab.com/en/adventures-in-statistics-2/multiple-regession-analysis-use-adjusted-r-squared-and-predicted-r-squared-to-include-the-correct-number-of-variables.
36. Carichner, G. *Square-Cube Law Revisited for Airships*. in *AIAA lighter-than-air systems technology (LTA) conference*. 2013.

``

CHAPTER 7: **Appendix**

7.1 Aircraft Classification

Aircraft			
S/No	**Category**	**Details**	**Count**
1	Utility Aircraft	Propellor driven single, two, four and, six-seater ultralight kit-built. Light utility transport, light utility turboprop, utility turboprop kit-built.	360
2	Agricultural Planes	Propellor driven Agricultural sprayers.	16
3	Sportplanes and Aerobatics	Propellor-driven Aerobatic single-seat, two-seater Sportplanes.	33
4	Amphibious Planes	One or two Propellor driven single, two, four, and six-seater amphibious aircraft.	18
5	Motor-glider	Propellor-driven single or two-seater motor-glider.	17
6	Fighters	Jet Multirole, Air superiority, and Attack Fighters	23

``

7	Trainer	Jet or turboprop-driven trainers.	27
8	Transport aircraft	Jet-driven wide-body airliner, Propeller-driven airliners.	54
9	Business Jet	Long-range business jets, supersonic business jets, and Private Jets	60
10	Freighters	Medium transport multirole, two or four turboprop driven Freighters.	18
Total			**626**

7.2 Rotorcraft Classification

S.No	Category	Count
1	Conventional	200
2	Fenestron	21
3	NOTAR	3
4	Coaxial Counter-Rotating	9
Total		233

7.3 Design Trends for Aircraft

MTOW Vs Wempty

``

MTOW Vs Wempty								Wempty=a*(MTOW) [b]			
	Overall	Airline	Fighter	Freighter	Business	Utility	Aerobatic	Amphibian	Trainer	Agricultural	Motor-glider
a	1.522	2.603	4.068	2.74	0.3161	0.5952	0.4601	0.1333	0.7337	0.5895	0.07663
b	0.9108	0.8682	0.7926	0.8579	1.052	0.9973	1.056	1.211	0.9787	0.9786	1.336
R-Sq	0.9959	0.9943	0.8913	0.9952	0.9885	0.9599	0.956	0.9701	0.9212	0.9597	0.9401
Max.E	72.03	51.37	24.82	63.43	37.33	78.30	21.59	17.27	88.71	31.93	40.56
Min.E	0.042	0.279	0.585	0.462	0.988	0.008	0.266	3.39	1.46	1.53	0.812
Avg.E	32.1	6.21	10.02	16.82	16.34	10.67	9.95	9.00	13.5	15.57	9.49
N	491	35	18	13	43	325	32	14	23	12	15

MTOW Vs Fuselage Length

MTOW Vs Length								Fuselage-Length=a*(MTOW) [b]			
	Overall	Jet Transport	Fighter	Freighter	Business	Utility	Aerobatic	Amphibian	Trainer	Agricultural	Motor-glider
a	0.5025	0.7234	0.4245	0.7928	0.4395	0.8447	0.8839	0.6315	0.79	1.537	0.8947
b	0.3847	0.3572	0.3722	0.3368	0.3966	0.317	0.3	0.363	0.41	0.2187	0.3252
R-Sq	0.9702	0.9539	0.7402	0.9738	0.974	0.822	0.7597	0.9593	0.9164	0.8429	0.7162
Max.E	62.9	28.85	21.18	22.18	47.23	38.16	12.27	16.29	16.51	8.54	12.07
Min.E	0.010	0.462	0.368	0.598	0.111	0.036	0.354	0.116	0.144	0.63	0.20
Avg.E	10.70	7.20	7.19	7.319	6.36	7.92	5.02	7.20	5.74	5.76	5.25
N	598	43	18	16	56	336	32	19	26	13	16

``

MTOW Vs Wingarea

MTOW Vs Wingspan								Wingspan=a*(MTOW) ^{b}			
	Overall excluding Fighter	Airline	Fighter	Freighter	Business	Utility	Aerobatic	Amphibian	Trainer	Agricultural	Motor-glider
a	1.131	0.5495	0.1515	1.982	1.028	1.954	3.893	1.223	6.541	2.394	1.688
b	0.3132	0.375	0.4324	0.261	0.3063	0.2423	0.1027	0.3124	0.0465	0.2257	0.3466
R-Sq	0.9508	0.967	0.794	0.9636	0.932	0.069	0.394	0.909	0.260	0.8078	0.795
Max.E	63.57	29.09	20.79	31.146	19.85	39.09	19.29	20.009	14.74	11.11	14.36
Min.E	0.719	0.917	0.588	0.040	0.52	0.060	0.159	0.022	0.259	0.332	0.095
Avg.E	13.80	6.96	8.20	6.27	7.25	9.58	5.81	7.27	5.89	6.84	5.43
N	569	51	20	16	52	335	31	19	22	13	12
Avg.E	48.49	10.00	15.44	8.91	14.77	14.96	0.263	14.72	10.80	12.61	14.02
N	485	39	17	12	40	305	32	15	21	12	15

MTOW Vs Wingarea

MTOW Vs Wingarea								Wing-Area=a*(MTOW) ^{b}			
	Overall	Airline	Fighter	Freighter	Business	Utility	Aerobatic	Amphibian	Trainer	Agricultural	Motor-glider
a	0.0271	0.0677	0.1887	0.1097	0.03393	1.035	2.617	0.2814	2.361	0.855	0.2712
b	0.7673	0.8697	0.5476	0.6435	0.7508	0.3896	0.205	0.5719	0.2395	0.4387	0.6258
R-Sq	0.966	0.975	0.689	0.995	0.954	0.7016	0.2618	0.9847	0.716	0.835	0.642
Avg.E	13.80	6.96	8.20	6.27	7.25	9.58	5.81	7.27	5.89	6.84	5.43
Max.E	78.13	33.62	36.65	13.81	37.09	53.82	36.65	37.80	30.18	34.98	23.65
N	569	51	20	16	52	335	31	19	22	13	12
Min.E	0.265	0.300	0.794	0.398	0.400	0.004	0.196	0.018	0.393	0.72	1.19
Avg.E	48.49	10.00	15.44	8.91	14.77	14.96	0.263	14.72	10.80	12.61	14.02
N	485	39	17	12	40	305	32	15	21	12	15

** For Overall aircrafts including Fighters R-sq is 0.8828, MAPE: 19.60 and Max error is 165.84% - Fighters show maximum deviation from trend line

MTOW Vs Wingspan

``

MTOW Vs Fuselage height

MTOW Vs Height								Height=a*(MTOW) ^{b}			
	Overall	Airline	Fighter	Freighter	Business	Utility	Aerobatic	Amphibian	Trainer	Agricultural	Motor-glider
a	0.2167	0.3262	0.5854	0.3802	0.3662	0.3203	0.9965	0.2245	0.3556	0.7777	0.783
b	0.3524	0.3202	0.2226	0.3082	0.2875	0.3034	0.1285	0.3554	0.2858	0.1624	0.142
R-Sq	0.961	0.944	0.632	0.9514	0.888	0.647	0.1304	0.913	0.943	0.430	0.128
Max.E	56.35	27.96	12.67	26.66	34.28	4.05	35.22	45.18	15.61	22.70	21.43
Min.E	0.08	0.078	0.05	0.10	0.127	0.09	1.55	0.87	0.27	0.48	5.72
Avg.E	13.18	7.80	5.59	8.87	8.24	11.85	13.41	13.26	5.23	10.55	13.25
N	543	49	18	16	53	302	23	15	22	11	11

MTOW Vs Power								POwer=a*(MTOW) ^{b}			
	Overall	Airline	Fighter	Freighter	Business	Utility	Aerobatic	Amphibian	Trainer	Agricultural	Motor-glider
a	0.0276	5×10^{-4}		1.1×10^{-2}	2.2×10^{-5}	0.0315	0.01629	0.08803	0.0419	0.0242	8×10^{-9}
b	1.196	1.606	N/A	1.273	2.149	1.211	1.388	1.073	1.206	1.22	4.266
R-Sq	0.993	0.9191	N/A	0.9968	0.863	0.9502	0.8536	0.9922	0.9436	0.9569	0.4366
Max.E	67.94	52.22	N/A	42.22	54.188	59.27	80.47	77.133	51.06	24.39	42387.3
Min.E	0.024	0.54	N/A	0.385	1.30	0.415	0.911	1.586	0.119	1.60	818.3
Avg.E	23.60	24.65	N/A	20.08	25.40	16.01	25.55	24.83	19.48	12.23	12553.3
N	461	6	N/A	14	11	334	29	19	12	16	16

MTOW Vs Power Available

``

MTOW Vs Thrust Available

MTOW Vs Thrust								Thrust=a*(MTOW) ^{b}			
	Overall	Airline	Fighter	Freighter	Business	Utility	Aerobatic	Amphibian	Trainer	Agricultural	Motor-glider
a	0.01752	6.818×10^{-3}	0.0137	N/A	8.619×10^{-3}	N/A	N/A	N/A	9.2×10^{-6}	N/A	N/A
b	0.8525	0.9274	0.9393		0.9074				1.723		
R-Sq	0.972	0.989	0.7466	N/A	0.989	N/A	N/A	N/A	0.7489	N/A	N/A
Max.E	68.93	25.04	59.9	N/A	40.71	N/A	N/A	N/A	51.33	N/A	N/A
Min.E	0.071	0.037	1.86	N/A	0..366	N/A	N/A	N/A	0.55	N/A	N/A
Avg.E	20.57	4.98	18.15	N/A	10.87	N/A	N/A	N/A	26.79	N/A	N/A
N	123	46	20	N/A	43	N/A	N/A	N/A	11	N/A	N/A

MTOW Vs Range								Range=a*(MTOW) ^{b}			
	Overall	Airline	Fighter	Freighter	Business	Utility	Aerobatic	Amphibian	Trainer	Agricultural	Motor-glider
a	75.63	3.804	87.95	13.32	70.77	40.18	91.5	149	50.08	28.57	70.89
b	0.4016	0.6399	0.3582	0.5317	0.4501	0.4987	0.3818	0.2794	0.4224	0.4283	0.4248
R-Sq	0.814	0.891	0.529	0.744	0.916	0.558	0.2223	0.526	0.6877	0.768	0.3348
Max.E	128.5	84.313	52.79	91.33	98.85	97.37	81.99	43.42	57.49	32.50	58.63
Min.E	0.070	0.014	0.706	9.555	0.057	0.216	4.366	2.42	0.2323	0.031	1.939
Avg.E	33.26	23.27	14.56	53.78	13.70	26.90	29.108	21.64	17.19	15.48	17.93
N	456	44	11	13	52	241	23	11	20	10	11

``

MTOW Vs Range

7.4 Design Trends for Rotorcrafts

RANK	S/NO	RELATION		Overall	Conv	F	CR	NOTAR
Very Strong Relationship > 0.70	1	MTOW Vs W_{empty} $W_{empty}=a\times(MTOW)^b$	**a**	0.8076	0.8069	0.4527	0.6395	0.1302
			b	0.9667	0.966	1.022	0.9988	1.179
			R.sq	0.9733	0.974	0.979	0.913	0.998
			Max. E	83.14	51.84	54.61	33.82	2.173
			Avg. E	12.91	11.73	10.35	13.82	1.432
			N	155	127	17	8	3
	2	MTOW Vs Main-Rotor-Diameter $RD=a\times(MTOW)^b$	**a**	0.7561	0.7661	1.509	1.199	0.5164
			b	0.3429	0.3428	0.2488	0.2775	0.3755
			R.sq	0.9177	0.9261	0.971	0.823	0.9274
			Max. E	48.317	27.60	11.57	55.78	4.077
			Avg. E	8.96	8.47	3.73	15.44	2.63
			N	162	135	17	7	3
	3	MTOW Vs Tail-Rotor-Diameter Tail $RD=a\times(MTOW)^b$	**a**	N/A	0.0726	0.1971	N/A	N/A
			b		0.4197	0.2049		
			R.sq	N/A	0.964	0.649	N/A	N/A
			Max. E	N/A	26.29	32.98	N/A	N/A
			Avg. E	N/A	7.92	12.10	N/A	N/A
			N	N/A	126	16	N/A	N/A
	4	MTOW Vs Blade-Area $B\text{-}Area=a\times(MTOW)^b$	**a**	Same	0.0135	N/A	N/A	N/A
			b		0.6254			
			R.sq	Same	0.9213	N/A	N/A	N/A
			Max. E	Same	39.20	N/A	N/A	N/A
			Avg. E	Same	16.03	N/A	N/A	N/A
			N	Same	23	N/A	N/A	N/A
	5	MTOW Vs F-Length	**a**	0.6492	0.6795	0.8686	0.8082	0.6556
			b	0.3522	0.3492	0.3143	0.2811	0.3422
			R.sq	0.9015	0.9373	0.977	0.991	0.8975

``

		Length=a×(MTOW)^b	**Max. E**	54.96	27.27	9.76	1.88	4.14
			Avg. E	8.21	6.63	3.68	1.37	2.90
			N	127	103	16	4	3
	6	MTOW Vs Height Height=a×(MTOW)^b	**a**	0.4774	0.4870	0.5074	0.6781	0.0496
			b	0.2456	0.2427	0.2318	0.2254	0.5391
			R.sq	0.8361	0.849	0.9506	0.911	0.873
			Max. E	25.86	25.51	7.42	5.64	8.34
			Avg. E	7.54	7.93	3.02	2.99	5.29
			N	96	81	8	4	3
	7	MTOW Vs Total-Takeoff-Power Tk-P=a×(MTOW)^b	**a**	0.1682	0.1645	0.0838	N/A	N/A
			b	1.06	1.062	1.144		
			R.sq	0.9454	0.9411	0.9815	N/A	N/A
			Max. E	98.99	78.97	68.46	N/A	N/A
			Avg. E	23.05	22.76	15.66	N/A	N/A
			N	65	53	10	N/A	N/A
	8	MTOW Vs Continuous-Power C-P=a×(MTOW)^b	**a**	1.08	1.14	2.337	N/A	N/A
			b	0.769	0.764	0.6715		
			R.sq	0.90	0.90	0.76	N/A	N/A
			Max. E	71.35	74.65	35.55	N/A	N/A
			Avg. E	19.92	21.62	14.40	N/A	N/A
			N	45	36	8	N/A	N/A
	9	MTOW Vs DiskLoading DL=a×(MTOW)^b	**a**	1.684	1.681	0.5915	0.03748	4.709
			b	0.3521	0.3492	0.4958	0.7952	0.2512
			R.sq	0.816	0.8422	0.9713	0.9268	0.5785
			Max. E	55.89	43.82	20.28	17.29	7.43
			Avg. E	16	15.46	7.45	8.88	5.33
			N	155	129	17	6	3
	10	MTOW Vs V_{MAX}	**a**	71.04	72.43	43.26	9.893	104.3
			b	0.1478	0.1446	0.2207	0.3628	0.1103
			R.sq	0.7115	0.71	0.9004	0.7297	0.5525
			Max. E	56.46	31.78	42.03	20.51	3.52

``

		Vmax=a×(MTOW)^{b}	**Avg. E**	10.13	9.59	10.57	10.59	2.40
			N	76	60	7	5	3
	11	Diskloading Vs Vmax Vmax=a×(DL)^{b}	**a**	69.52	67.06	54.15	39.65	53.9
			b	0.3643	0.3781	0.4469	0.4828	0.4334
			R.sq	0.7889	0.7744	0.9379	0.9284	0.9988
			Max. E	41.51	35.39	30.08	7.42	0.1741
			Avg. E	8.37	8.36	8.54	4.18	0.108
			N	76	60	7	5	3
	12	Wempty Vs Main-Rotor-Diameter DL=a×(Wempty)^{b}	**a**	0.9234	0.93	1.596	1.249	1.282
			b	0.3404	0.3413	0.2601	0.2976	0.2817
			R.sq	0.9234	0.9282	0.9169	0.9053	0.9312
			Max. E	38.31	26.96	27.48	47.51	5.61
			Avg. E	8.70	8.38	6.419	11.75	2.72
			N	150	121	17	7	4
	13	Main-Rotor-Diameter Vs Takeoff-Power. TP=a×(RD)^{b}	**a**	0.6721	0.3791	0.0109	N/A	N/A
			b	2.906	3.091	4.651		
			R.sq	0.6847	0.683	0.906	N/A	N/A
			Max. E	269	265.55	43.12	N/A	N/A
			Avg. E	58.64	49.54	23	N/A	N/A
			N	65	53	10	N/A	N/A
	14	Main-Rotor-Diameter Vs Blade Area. B-Area=a×(RD)^{b}	**a**	0.0449	N/A	N/A	N/A	N/A
			b	1.595				
			R.sq	0.5946	N/A	N/A	N/A	N/A
			Max. E	98.9	N/A	N/A	N/A	N/A
			Avg. E	80.94	N/A	N/A	N/A	N/A
			N	29	N/A	N/A	N/A	N/A
	15	Main-Rotor-Diameter Vs Length Length=a×(RD)^{b}	**a**	0.8882	0.9065	0.5871	0.1039	1.60
			b	1.014	1.0122	1.211	1.686	0.7769
			R.sq	0.9147	0.9555	0.985	0.923	0.680
			Max. E	54.24	7.65	6.23	11.11	3.95
			Avg. E	8.60	6.54	2.75	3.19	2.39

``

			N	129	104	15	7	3
	16	Main-Rotor-Diameter Vs Height Height=a×(RD)^{b}	**a**	0.5328	0.5226	0.4715	0.1235	0.1233
			b	0.7569	0.7567	0.8038	1.371	1.453
			R.sq	0.8505	0.899	0.881	0.99	0.989
			Max. E	23.44	21.02	14.74	2.14	3.657
			Avg. E	7.36	6.78	3.71	0.843	1.422
			N	98	81	8	6	3
	17	Main-Rotor-Diameter Vs Tail-Rotor-Diameter. Tail-RD=a×(RD)^{b}	**a**	N/A	0.1312	0.1931	N/A	N/A
			b		1.127	0.7058		
			R.sq	N/A	0.928	0.709	N/A	N/A
			Max. E	N/A	35.82	34.01	N/A	N/A
			Avg. E	N/A	8.75	10.13	N/A	N/A
			N	N/A	128	14	N/A	N/A
	18	Tail-Rotor-Diameter-Vs-Length Length=a×(T-RD)^{b}	**a**	6.847	6.068	10.42	N/A	N/A
			b	0.7225	0.8212	0.8948		
			R.sq	0.8296	0.70	0.9092	N/A	N/A
			Max. E	50.48	34.40	33.36	N/A	N/A
			Avg. E	12.58	14	8.587	N/A	N/A
			N	11	98	13	N/A	N/A
	19	Tail-Rotor-Diameter Vs Height Height=a×(T-RD)^{b}	**a**	2.456	2.225	3.311	N/A	N/A
			b	0.4896	0.5714	0.5433		
			R.sq	0.759	0.8437	0.913	N/A	N/A
			Max. E	35.46	31.33	12.81	N/A	N/A
			Avg. E	10.04	7.59	3.94	N/A	N/A
			N	87	79	8	N/A	N/A
	20	Takeoff-Power Vs V_{max} Vmax=a×(TK-P)^{b}	**a**	94.84	97.75	80.42	31.81	N/A
			b	0.1323	0.127	0.1685	0.2737	
			R.sq	0.78	0.79	0.8254	0.9415	N/A
			Max. E	51.97	26.30	47.4	9.26	N/A
			Avg. E	9.08	8.021	14.08	1.67	N/A
			N	65	51	6	6	N/A
	21		**a**	356.6	336.9	533.2	755	N/A
			b	-0.3	-0.256	-0.641	-0.777	

``

		Powerloading Vs V_{max} $Vmax=a\times(PL)^b$	**R.sq**	0.3162	0.257	0.5922	0.9862	N/A
			Max. E	106.01	55.13	68.772	5.15	N/A
			Avg. E	15.03	14.85	19.28	2.21	N/A
				65	51	6	6	N/A
	22	Main-Rotor-Diameter Vs Vmax $Vmax=a\times(RD)^b$	**a**	88.96	88.48	32.45	92.66	154.4
			b	0.3897	0.3861	0.8547	0.3923	0.2036
			R.sq	0.5242	0.5562	0.8318	0.030	0.271
			Max. E	79.78	36.60	55.47	30.47	4.26
			Avg. E	13.66	12.24	12.68	16.03	2.80
			N	76	60	7	5	3
Statistically Insignificant	1	TAIL DIAMETER VS ENDURANCE						
	2	BLADEAREA VS ENDURANCE						
	3	BLADEAREA VS ROC						
	4	RANGE VS ROC						
	5	ENDURANCE VS SERVICECEILING						
	6	ENDURANCE VS ROC						
	7	ENDURANCE VS V_{MAX}						
	8	ENDURANCE VS V_{CRUISE}						
	9	SERVICECEILING VS ROC						
	10	MTOW VS ENDURANCE						